

RESEARCH ARTICLE

Population genomics and geographic dispersal in Chagas disease vectors: Landscape drivers and evidence of possible adaptation to the domestic setting

Luis E. Hernandez-Castro^{1,2*}, Anita G. Villacís³, Arne Jacobs^{1,4}, Bachar Cheaib¹, Casey C. Day⁵, Sofía Ocaña-Mayorga³, Cesar A. Yumiseva³, Antonella Bacigalupo¹, Björn Andersson⁶, Louise Matthews¹, Erin L. Landguth^{5,7}, Jaime A. Costales³, Martin S. Llewellyn^{1,8*}, Mario J. Grijalva^{3,8}

1 Institute of Biodiversity, Animal Health and Comparative Medicine, University of Glasgow, Glasgow, United Kingdom, **2** The Epidemiology, Economics and Risk Assessment Group, The Roslin Institute, Easter Bush Campus, The University of Edinburgh, Midlothian, United Kingdom, **3** Centro de Investigación para la Salud en América Latina, Facultad de Ciencias Exactas y Naturales, Pontificia Universidad Católica del Ecuador, Quito, Ecuador, **4** Department of Natural Resources and the Environment, Cornell University, Ithaca, New York, United States of America, **5** Computational Ecology Lab, School of Public and Community Health Sciences, University of Montana, Missoula, Montana, United States of America, **6** Department of Cell and Molecular Biology, Karolinska Institutet, Stockholm, Sweden, **7** Center for Population Health Research, School of Public and Community Health Sciences, University of Montana, Missoula, Montana, United States of America, **8** Infectious and Tropical Disease Institute, Department of Biomedical Sciences, Heritage College of Osteopathic Medicine, Ohio University, Athens, Ohio, United States of America

✉ These authors contributed equally to this work.

* enriqhernandez18@gmail.com (LEH-C); martin.llewellyn@glasgow.ac.uk (MSL)

Abstract

Accurate prediction of vectors dispersal, as well as identification of adaptations that allow blood-feeding vectors to thrive in built environments, are a basis for effective disease control. Here we adopted a landscape genomics approach to assay gene flow, possible local adaptation, and drivers of population structure in *Rhodnius ecuadoriensis*, an important vector of Chagas disease. We used a reduced-representation sequencing technique (2b-RAD-seq) to obtain 2,552 SNP markers across 272 *R. ecuadoriensis* samples from 25 collection sites in southern Ecuador. Evidence of high and directional gene flow between seven wild and domestic population pairs across our study site indicates insecticide-based control will be hindered by repeated re-infestation of houses from the forest. Preliminary genome scans across multiple population pairs revealed shared outlier loci potentially consistent with local adaptation to the domestic setting, which we mapped to genes involved with embryogenesis and saliva production. Landscape genomic models showed elevation is a key barrier to *R. ecuadoriensis* dispersal. Together our results shed early light on the genomic adaptation in triatomine vectors and facilitate vector control by predicting that spatially-targeted, proactive interventions would be more efficacious than current, reactive approaches.



OPEN ACCESS

Citation: Hernandez-Castro LE, Villacís AG, Jacobs A, Cheaib B, Day CC, Ocaña-Mayorga S, et al. (2022) Population genomics and geographic dispersal in Chagas disease vectors: Landscape drivers and evidence of possible adaptation to the domestic setting. PLoS Genet 18(2): e1010019. <https://doi.org/10.1371/journal.pgen.1010019>

Editor: Giorgio Sirugo, University of Pennsylvania, UNITED STATES

Received: July 12, 2021

Accepted: January 6, 2022

Published: February 4, 2022

Peer Review History: PLOS recognizes the benefits of transparency in the peer review process; therefore, we enable the publication of all of the content of peer review and author responses alongside final, published articles. The editorial history of this article is available here: <https://doi.org/10.1371/journal.pgen.1010019>

Copyright: © 2022 Hernandez-Castro et al. This is an open access article distributed under the terms of the [Creative Commons Attribution License](https://creativecommons.org/licenses/by/4.0/), which permits unrestricted use, distribution, and reproduction in any medium, provided the original author and source are credited.

Data Availability Statement: *Rhodnius ecuadoriensis* 2b-RAD raw sequence reads are stored in the Sequence Read Archive (SRA)

repository accession number PRJNA797230 R code is available at the Github repository: github.com/lehernandezc/recuadoriensis.

Funding: This work was possible thanks to the Mexican Council of Science and Technology (conacyt.mx/) doctorate scholarship (CVU Number 613766) awarded to LEHC., the National Institutes of Health (NIH - www.nih.gov) grant number R15 AI105749-01A1 allocated to MJG who is PI, as well as together with MSL the UKRI (www.ukri.org/councils/) Engagement Network (EP/T003782/1) which supported co-author interactions. Funding was also received from Pontifical Catholic University of Ecuador (www.puce.edu.ec) to MJG (grant # C13025, E13027, E13037, H13174, I13048). ELL was supported by the National Institute of General Medical Sciences of the NIH (www.nih.gov), United States (Award Numbers P20GM130418). The funders had no role in study design, data collection and analysis, decision to publish, or preparation of the manuscript.

Competing interests: The authors have declared that no competing interests exist.

Author summary

Re-infestation of recently insecticide-treated houses by wild/secondary triatomine, their potential adaptation to this new environment and capabilities to geographically disperse across multiple human communities jeopardise sustainable Chagas disease control. This is the first study in Chagas disease vectors that identifies genomic regions possibly linked to adaptations to the built environment and describes landscape drivers for accurate prediction of geographic dispersal. We sampled multiple domestic and wild *Rhodnius ecuadoriensis* population pairs across a mountainous terrain in southern Ecuador. We evidenced that triatomine movement from forest to built environments does occur at a high rate. In these highly connected population pairs we detected loci possibly linked to local adaptation among the genomic makers we evaluated and in doing so we pave the way for future triatomine genomic research. We highlighted that current haphazardous vector control in the zone will be hindered by reinfestation of triatomines from the forest. Instead, we recommend frequent and spatially-targeted vector control and provided a landscape genomic model that identifies highly connected and isolated triatomine populations to facilitate efficient vector control.

Introduction

The process by which insect vectors of human diseases adapt to survive and breed in human habitats is fundamental to the emergence and spread of vector-borne diseases (e.g., *Aedes aegypti* [1]). Relatively modest changes in vector host preference between ancestral (wild) and derived (domesticated) forms can drive devastating epidemics that result in millions of deaths [2]. Host preference variability in *Culex pipiens* of hybrid ancestry is thought to be genetically based and has contributed to local West Nile virus outbreaks in North America [3,4]. Similarly, host choice behaviour in Malaria mosquito *Anopheles arabiensis* has been linked to the allelic variation of a 3Ra chromosomal inversion [5]. Understanding the evolution and genetic bases of traits associated to the domestic habitat in disease vectors is, therefore, paramount and could inform control efforts and reveal the epidemic potential for new vector species [6,7].

Triatominae (Hemiptera: Reduviidae) are a group of hematophagous arthropods that transmit *Trypanosoma cruzi*, the parasite that causes Chagas disease, a fatal parasitic infection afflicting more than seven million people in Latin America [8]. Approximately 20 species are of public health concern due to their involvement in *T. cruzi* domestic transmission [9]. Eradication of ‘domesticated’ triatomines through insecticide spraying has been the mainstay of disease control in the past (e.g., *Triatoma infestans* [10], *Rhodnius prolixus* and *Triatoma dimidiata* [11]). However, wild (e.g., *T. infestans* [12] and *R. prolixus* [13]) and/or secondary competent species of triatomines (e.g., *Triatoma sordida* [14], *Triatoma maculata* and *Rhodnius pallescens* [15], *Panstrongylus howardi* [16] and *P. chinai* [17]) can continuously occupy empty domestic niches. Except from a few species that intrude houses seasonally (e.g., *Triatoma dimidiata* and other species in the Amazon basin [18,19]), constant triatomine house colonisation has historically jeopardised Chagas disease control strategies.

Colonisation of the domestic niche may involve multiple, independent evolutionary processes across the geographic distribution of a given vector species [20,21], analogous to parallel trophic speciation observed in other arthropods [22]. Alternatively, domestication (hereafter, refers to the long-term evolutionary sense) of vectors with their associated zoonotic parasites may result from a single or limited number of independent colonisation events, followed by rapid and widespread dispersal within the domestic setting [23,24]. Domestication, and

selection for domestic traits (e.g., pathogen resistance or efficient pollinators), in a given species may also represent a combination of these two scenarios, where multiple domesticated lineages serially introgress with wild lineages over evolutionary time, as has been elegantly demonstrated through analysis of the genomes of the *Scutellata*-European hybrid honey bees in America [25,26]. Disentangling these different scenarios in triatomine species, and their important implications for disease control, has been challenging due to a lack of genomic resources for these organisms which are only recently becoming available [27–29]. With adequate genomic tools; however, patterns of colonisation of the domestic niche can be established, and their underlying mechanisms unveiled. Models of ‘adaptation with gene flow’ (e.g., [30]) exploit standard population genetic metrics and theory to make generalisations about the genomic basis of adaptations (e.g., [22]). Such models can be deployed to study disease vector colonisation and reveal fundamental traits associated with the domestic niche.

The genetic changes that allowed triatomines to thrive in the domestic niche may be related to feeding, reproduction and developmental performance. For instance, the development of potent saliva compounds that alter vertebrate host homeostatic, anti-inflammatory and immune responses was a crucial adaptation in triatomines for successful blood intake, and therefore, survival [31,32]. Saliva composition variation between domestic and wild populations has not been shown, yet saliva composition does play a role in highly ‘domesticated’ triatomines (e.g., *R. prolixus* and *T. infestans*) with exceptional feeding performance in humans [33,34]. Morphological changes such as reduced sexual dimorphism and body size have also been associated with the domestic habitat [35]. Egg development and viability are driven by neurohormonal signaling pathways starting soon after a female feeds on blood which results in yolk formation and supports embryonic development [36]. Under laboratory conditions, embryonic development of eggs collected inside houses was faster than those from the peridomicile [37]. Morphometric studies have attempted to develop phenotypic markers in triatomines associated with domestic or wild ecotopes with little (e.g., [38]) to moderate (e.g., [39]) success. Therefore, association of triatomine with the domestic niche is currently a qualitative concept with urgent need for quantitative foundations [40].

Identification of the ecological factors driving triatomine dispersal, with subsequent colonisation of a given niche, is necessary to predict complex triatomine population dynamics. High localised genetic structuring is expected in triatomine populations given their poor flying capabilities (< 2 Km), nymphs can only crawl short distances, and long-distance dispersal may sporadically occur via attachment to human cloths/bird feathers [41–43]. Models based on presence-only data have shown altitude, temperature, humidity, precipitation and vegetation as important variables for triatomine distribution [44–46]. These models, however, represent broad spatial distribution rather than detailed local vector population dynamics and their accuracy requires extensive entomological records [47–49]. Instead, a landscape genomics framework (Fig 1) can accurately define landscape functional connectivity (the level at which the landscape heterogeneity facilitates or impedes a given organism’s movement from, and to, different habitat patches [50]) and shed light on the drivers of dispersal in a given vector species, and even assist in identifying poorly connected or isolated areas that can be easily targeted by eradication interventions [51–53]. Elevation may be a factor limiting *R. ecuadoriensis* dispersal given it limits the presence of other triatomine species [46]. Habitat fragmentation and human agricultural activities have shown to have an effect on triatomine population dynamics [54]. Human-mediated passive triatomine dispersal has been suggested elsewhere [11,41–43], and therefore, we assume roads might connect triatomine populations (Fig 1D).

Rhodnius ecuadoriensis is the major vector for Chagas disease in Ecuador and Northern Peru [55]. Both domestic and wild populations of this species exist throughout its range [56]. Preliminary morphological and genetic evidence suggests some gene flow of *R. ecuadoriensis*

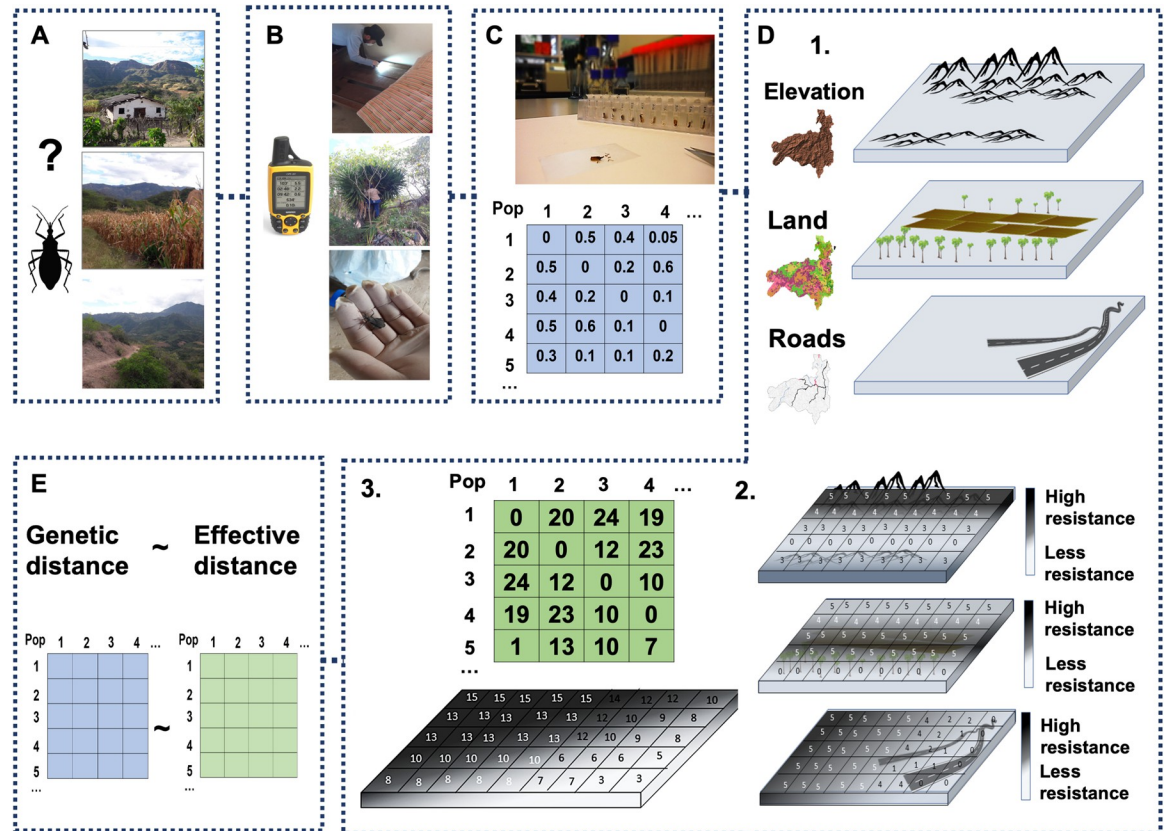


Fig 1. Step-by-step walk-through of the landscape genomics mixed modelling framework used to study the Chagas disease arthropod vector, *Rhodnius ecuadoriensis*. A, First, a research question is defined based on whether gene flow or adaptation processes are to be investigated and sampling design is established. B, In the field, triatomines are collected in different ecotopes in the spatial and temporal gradients defined in A. Different variables are recorded at this stage such as altitude and geographic coordinates. C, In the laboratory, triatomine next generation sequencing (NGS) libraries are prepared and sequenced in high-throughput platforms. NGS data is processed with bioinformatic tools, and each sample genotype information is used to obtain a matrix of pairwise populations (Pop) genetic distances. D, A hypothetical landscape model (1) is parametrised into a resistance surface (2) which is a spatial representation of a given species movement constraints at each grid cell on a digital layer. From this resistance surface, a matrix of pairwise population (Pop) effective distances is calculated (3). E, Finally, statistical methods are used to correlate pairwise population genetic and effective distance matrices to investigate whether isolation-by-resistance (landscape functional connectivity) is a fitted model of the genetic differentiation of triatomine populations. Source maps: www.usgs.gov/centers/eros/science/usgs-eros-archive-digital-elevation-global-multi-resolution-terrain-elevation, www.usgs.gov/media/images/south-america-land-cover-characteristics-data-base-version-20 and dataportal.pbl.nl/downloads/GRIP4/GRIP4_Region2_vector_shp.zip.

<https://doi.org/10.1371/journal.pgen.1010019.g001>

between domestic and wild ecotopes [57,58]. By comparison, genetic studies of *T. cruzi* infecting the same vectors in Ecuador have shown strong to moderate differentiation between wild and domestic isolates [59,60]. As such there is a lack of a clear understanding of the micro and macro-evolutionary and ecological forces shaping *R. ecuadoriensis* domestic adaptation and dispersal capabilities, and those of the parasites they transmit.

Our study represents an attempt to evidence gene flow from wild to domestic ecotopes in *R. ecuadoriensis* in Ecuador, a preliminary survey of any potential genomic signatures of adaptation to the domestic niche in triatomines, as well as an assessment of the landscape drivers of vector dispersal. We used a reduced-representation sequencing approach (2b- RADseq) to recover genome-wide SNP variation in 272 *Rhodnius ecuadoriensis* individuals collected across ecological gradients in Loja, Ecuador. We confirmed *R. ecuadoriensis* do frequently invade houses from the forest in southern Ecuador. Significantly elevated allelic richness in wild sites

by comparison to nearby domestic foci clearly confirmed that dispersal occurred most frequently from wild ecotopes into domestic structures. Genome scans across multiple parallel colonisation events revealed possible evidence of ‘adaptation with gene flow’, with key outlier loci associated with colonisation of built domestic structures and, presumably, human blood feeding. Several outlier loci were mapped to the annotated regions of the *R. prolixus* genome. A strong signature of isolation-by-distance (IBD) was observable throughout the dataset, an effect less pronounced between domestic sites than between wild foci. Formal landscape genomic analyses revealed elevation surface as the major barrier to genetic connectivity between populations. Landscape genomic analysis enabled a spatial model of vector connectivity to be elaborated, informing ongoing control efforts in the region and providing a model for mapping the dispersal potential of triatomines and other disease vectors. Our findings suggest frequent and spatially targeted interventions, to cope with high gene flow and fragmented populations, are necessary to suppress Chagas disease transmission in Loja. Moreover, the discovery of signatures of possible local adaptation shed the first light on the genomic basis of domestication in triatomines.

Results

Recovery of SNP markers from 272 *Rhodnius ecuadoriensis* SNP specimens

Our CspCI-based 2b-RAD protocol was successful in obtaining genome-wide SNP information for *R. ecuadoriensis*. Sequencing of non-target species was minimal (0.2%). We genotyped six *Rhodnius prolixus* as controls and 80% of reads mapped to the *R. prolixus* reference genome. Only 9.5% of *R. ecuadoriensis* reads mapped to the same reference, a consequence of genomic sequence divergence between *R. ecuadoriensis* and *R. prolixus* [61] (S1 Methods). A stringent genotyping approach confidently identified 2,552 SNP markers across 272 *R. ecuadoriensis* samples from 25 collection sites, which represented closely administrative boundaries of human communities. In seven collection sites (Fig 2A; CG, BR, CE, CQ, HY, SJ and GL—seven pairs) triatomines from both domestic and wild ecotopes were collected. Remaining sites only had individuals of one ecotope (domestic or wild; S1 Table).

Reduced *R. ecuadoriensis* population genetic diversity in domestic ecotopes

Multiple genetic diversity estimates among populations from the 25 collection sites in Loja province were calculated (observed heterozygosity (H_O), gene diversity (H_E), inbreeding coefficient (F_{IS}) and allelic richness (A_r)). Diversity estimates ranged from 0.11 to 0.23, from 0.09 to 0.22, and from -0.24 to 0.11 for H_O , H_E and F_{IS} , respectively. Sample-size corrected A_r values ranged from 1.19 to 1.44 with the lowest values in La Extensa (EX), San Jacinto (SJ), El Huayco (HY) and Santa Rita (RT). In the paired ecotopes within the seven collection sites, A_r values were significantly higher for wild than domestic triatomine populations and in five out of seven instances ($p < 0.05$, rarefaction method [62]; S2 Table).

Genomic differentiation between domestic and wild ecotopes

To assay population dynamics between sympatric domestic and wild foci, we focused our individual-based genomic differentiation and pairwise F_{ST} comparisons analyses on the seven collection sites for which samples from both ecotopes were available (Fig 2A). Supporting frequent migration between domestic and wild ecotopes, samples from each ecotope were interleaved at most collection sites in the phylogenetic tree, with collection site geography, not ecotope, impacting the tree topology (Fig 2B). As such, samples collected in Galapagos (GL), Coamine (CE) and Chaquizhca (CQ) formed distinct clusters, and El Huayco (HY)—San

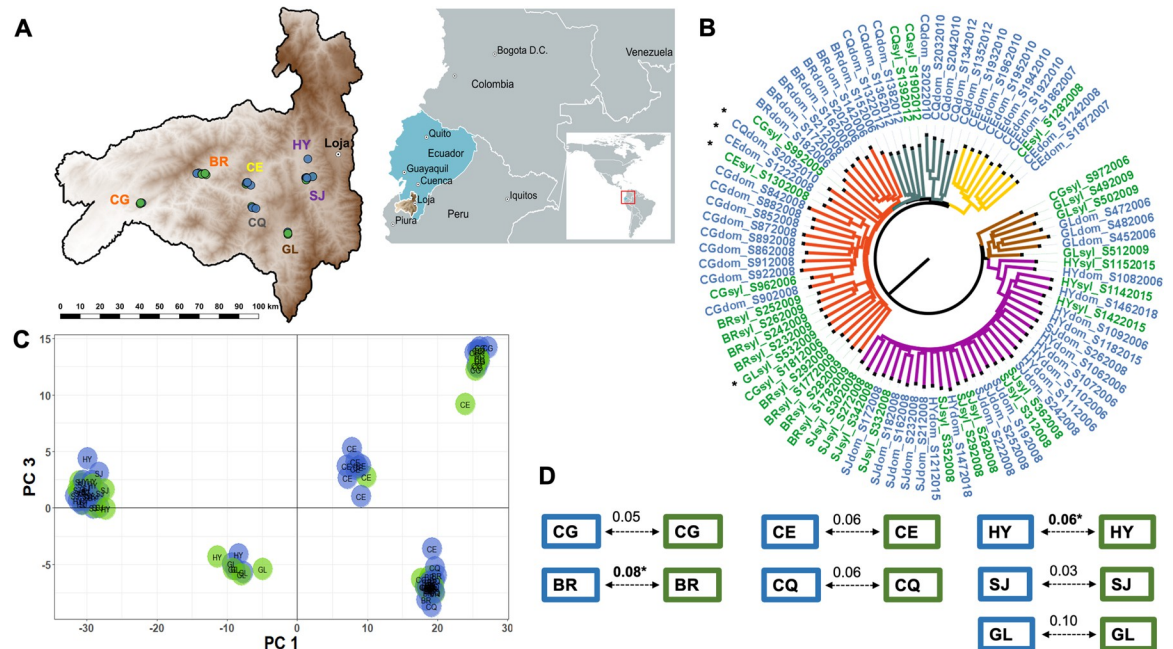


Fig 2. Genomic differentiation of domestic and wild *R. ecuadoriensis*. A, geographic distribution of the seven collection sites with both ecotypes over an elevation surface map of Loja. B, Neighbor-Joining midpoint phylogenetic tree with phylogenies indicating the Euclidean distance between triatomine samples built from allele counts. Tree branches clades are colour-coded to differentiate geographic collection sites (or clusters of collection sites) including some apparent migrants (black asterisks). Branch tip labels are coloured to indicate ecotype (domestic—blue / wild—green). C, the scatter plot shows five clusters are built with the first and third principal components of the discriminant analysis eigenvalues. D, pairwise F_{ST} comparisons between domestic (blue box) and wild (green box) *R. ecuadoriensis* in multiple sites across Loja (A). Significant F_{ST} values (arrows) after FDR correction are highlighted in bold and an asterisk. In all panels, samples location (dots) and labels are colour-coded to indicate their domestic (blue) or wild (green) collection ecotype. Collection sites abbreviations: SJ, San Jacinto; HY, EL Huayco; GL, Galapagos; CQ, Chaquizhca; CE, Coamire; BR, Bramaderos; CG, La Cienega (see S1 Table for full collection sites list). Source map: www.usgs.gov/centers/eros/science/usgs-eros-archive-digital-elevation-global-multi-resolution-terrain-elevation.

<https://doi.org/10.1371/journal.pgen.1010019.g002>

Jacinto (SJ) and Bramaderos (BR)—La Cienega (CG) also grouped discretely. Five broadly congruent clusters were defined in a discriminant analysis of principal components (DAPC) (Fig 2C), with geographic collection site rather than ecotype (silvatic vs domestic) again structuring observed diversity. F_{ST} indices between paired domestic and wild triatomine samples within each of the seven compared collection sites indicate little differentiation (e.g., $F_{ST} \leq 0.10$). Permutation tests indicated that F_{ST} was significant ($p < 0.05$) at only two sites—Bramaderos and El Huayco (Fig 2D). As expected, hierarchical analysis of molecular variance revealed genetic subdivision was significantly stronger ($F_{collection\ sites/total} = 0.26$, $p\text{-value} < 0.001$) among collection sites than among ecotypes within collection sites ($F_{ecotope/collection\ site} = -0.004$, $p\text{-value} < 0.001$) or among collection year within communities ($F_{collection\ year/collection\ site} = 0.06$, $p\text{-value} < 0.001$) (S3 Table).

Genetic loci correlated with domestic colonisation

To identify loci among our markers associated with domestic colonisation, we combined a Random Forest (RF) classification approach and redundancy analyses (RDA) with outlier scans (see Methods). We included the seven collection sites with frequent domestic-wild migration and three additional wild-only sites to roughly conform similar number of domestic ($n = 56$) and wild ($n = 52$) samples. A total of 347 SNPs provided high ranked classification accuracy (mean > 3) across the three RF iterations (inset in Fig 3A). Backwards purging on this highly discriminatory subset of SNPs detected a set of 43 SNPs that minimised the ‘Out-

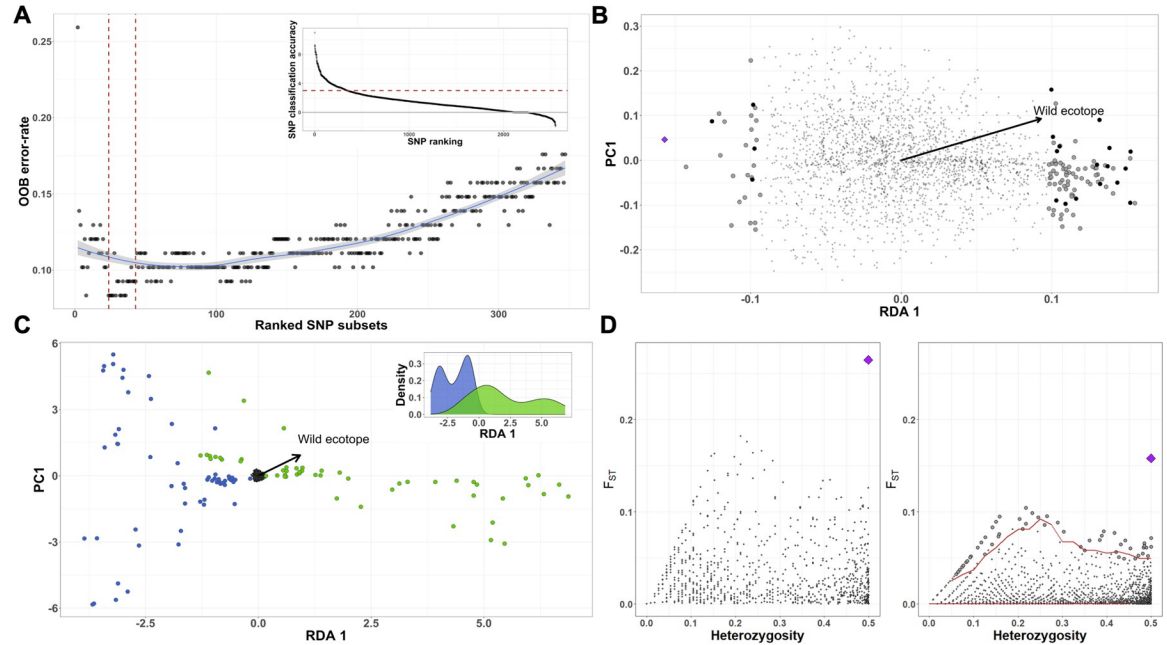


Fig 3. Scanning outlier SNP markers for signatures of local adaptation in *Rhodnius ecuadoriensis*. **A**, Random Forest backwards purging shows subsets with decreasing number of highly discriminatory SNPs and their resulting OOB-ER. The two vertical red lines indicated the 43 SNPs subset with the lowest OOB-ER and maximum discriminatory power between domestic and wild ecotopes. The inset shows SNPs ranked based on their classification accuracy averaged after 3-independent RF runs. SNPs with classification accuracy above three (red horizontal line) were used for the backwards purging. **B**, In our RDA model, SNPs (dots and diamonds) are arranged as a function of their relationship with the constrained predictor (RDA 1), ecotope (arrow outlines towards a wild ecotope relationship). SNPs closer to the centre (small grey dots) are not showing relation with the predictor. Outlier loci/SNPs are represented by those large dots/diamond loading at ± 2 SD and ± 3 SD separated from the mean SNPs loading distribution and showing a strong relationship with ecotope. Black large dots (and purple diamond) represent loci/SNP identified with high classification power in RF analysis. **C**, a biplot of *R. ecuadoriensis* triatomine samples and SNPs (small black dots in the centre) are arranged in relation to the constrained RDA axis with an arrow indicating those related to the wild ecotope. Dots are colour-coded to show sample ecotope of collection, domestic (blue) or wild (green). Biplot scaling is symmetrical with inset showing the density function for the RDA axis. **D**, Scatter plots show OutFlank (left) and fsthet (right) SNPs F_{ST} -heterozygosity relationship. 43 SNPs (large dots) had higher than average F_{ST} distribution of neutral loci in fsthet, whereas only one in OutFlank. Purple diamond indicated the SNP (ID 15732) flagged in all four analyses.

<https://doi.org/10.1371/journal.pgen.1010019.g003>

of-bag' error rate (OOB-ER) to 0.09 and maximised the discriminatory power among domestic and wild samples (Fig 3A). In a parallel RDA model, ecotope (domestic / wild) was a predictor explaining approximately 0.4% of the total variation and the constrained axis built from that variation was significant (p-value < 0.001), and so was the full model as indicated by the Monte Carlo permutation test. The distribution of each SNP loading/contribution to the RDA significant axis showed 109 candidate outlier loci as SNPs loadings at ± 2 SD from the mean of this distribution (permissive threshold; Fig 3B). In a more conservative approach, we also identified seven loci from those 109 under very strong selection as represented by those SNPs loading at the extreme ± 3 SD (conservative threshold) away from the mean distribution of the constrained axis (Fig 3B). The arrangement of the individual samples in the ordination space with relation to the RDA axis showed a clear pattern of subdivision comparable to the ecotope in which samples were collected (Fig 3C). The 21 loci/SNPs identified as outlier loci (dark dots in Fig 3B) by RDA were also detected as highly discriminatory SNPs for domestic and wild ecotopes in the RF analysis. Assuming 'adaptation with gene flow' we assessed locus-specific estimates of F_{ST} (Fig 3D), among the 2552 SNPs between domestic and wild ecotopes and identified one SNP (Locus ID 15732 –purple diamond in Fig 3B and 3D) possibly under local adaptation and/or spatial heterogeneous selection as suggested by OutFlank analysis (Fig 3D

left). Moreover, outlier scan with *fsthet* (Fig 3D right) in the same subset flagged this OutFlank SNP and 73 additional SNPs showing F_{ST} higher than the average neutral loci distribution at a 5% threshold. In summary, 43 SNPs were identified with the highest classification accuracy in RF analysis. 21 of those SNPs showed some signal of selection (that is, loaded ± 2 SD away from mean distribution of the constrained axis) and four were identified showing strong signal of selection (that is, loaded ± 3 SD away from the mean distribution of the constrained axis) in RDA analysis. Three of the SNPs flagged as outliers in *fsthet* analysis were found also being at high classification accuracy in RF analysis. The SNP (Locus ID 15732) possibly under strong selection as identified by OutFlank analysis, also had a high classification accuracy in RF and, interestingly, it was also identified within the RDA and *fsthet* SNPs sets as under a strong signal of selection.

Mapping outlier loci to the *Rhodnius prolixus* genome

Several outlier SNPs from the different analyses mapped to annotated regions of the *R. prolixus* genome. One SNP identified in the RDA analysis mapped (97.1% identity) in a *R. prolixus* genome region containing the characterised *Krüppel* gap gene (Accession No JN092576.1) involved in arthropod embryonic development [63]. Three outlier SNPs identified in *fsthet* analysis mapped (100% identity) to regions in the *R. prolixus* genome containing characterised GE-rich and polylysine protein precursors (mRNA—Accession AY340265.1), and the *Krüppel* and giant gap genes [63,64] (Accession No HQ853222.1). The former are important proteins within the sialome of blood-sucking bugs [65] and the latter involved in arthropod embryonic development [64]. Mapping of the majority of putatively outlier SNPs, including Locus ID 15732, was not possible in the absence of an available *R. ecuadoriensis* genome.

Comparison of dispersal rates of *R. ecuadoriensis* between domestic sites with dispersal rates between wild sites

Including all samples ($n = 272$) and collection sites ($n = 25$), we tested the strength of genetic isolation-by-distance (IBD) initially among domestic sample collection sites and latterly among wild collection sites (Fig 4). Mantel tests in both domestic ($r_m = 0.46$, p -value < 0.001) and wild ($r_m = 0.31$, p -value = 0.043) ecotopes strongly supported an effect of geographic distance on genetic distance (Fig 4A). Based on a generalised least square model with maximum likelihood population effects parametrisation (GLS-MLPE), the effect of geographic distance was significantly stronger (0.0018, p -value < 0.001) in wild compared to domestic foci (Fig 4A), suggesting that the rate of vector dispersal occurred at a higher rate between domestic populations than between wild ones (S4 Table).

Landscape functional connectivity in *R. ecuadoriensis*

Landscape genomic mixed modelling aims to identify the effect of different combinations of landscape surfaces and their parameters on a given genomic differentiation pattern (see Methods). *R. ecuadoriensis* genomic differentiation was closely partitioned by collection sites (Fig 5A) which was evidenced through hierarchical (S3 Table), phylogenetic, DAPC (Fig 2) and Admixture analyses (S1 and S2 Figs). To obtain an accurate representation of the genomic differentiation pattern among *R. ecuadoriensis* populations, we chose Hedrick's G_{ST} pairwise comparisons (Fig 5B) which corrects for sampling limited number of populations [66]. The genomic pattern was consistent regardless of metric used (e.g., Pairwise F_{ST} [67] and Meirman's standardised F_{ST} [68]) as revealed by strong and significant ($r^2 = 0.99$ & 0.92 , respectively; $p < 0.001$) Pearson's correlations between them. Pairwise Hedrick's G_{ST} comparisons (Fig 5B) showed a strong pattern of population structure across Loja province with presence of

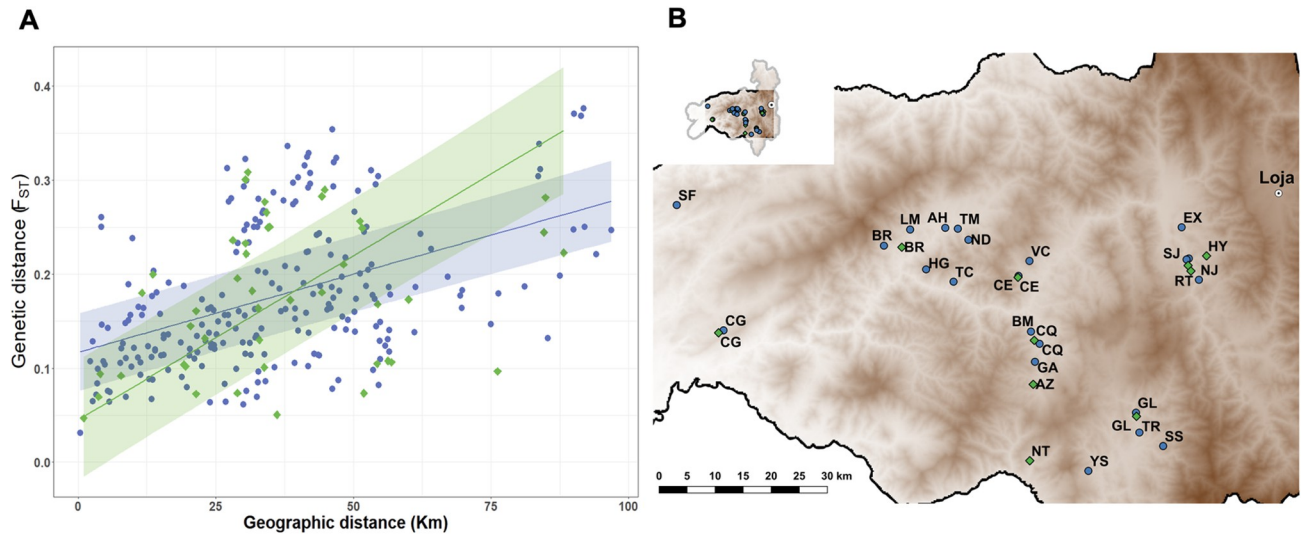


Fig 4. Dispersal rate in *R. ecuadoriensis*. A, correlation between pairwise genetic (F_{ST}) and geographic distances (data points) with fitted regression lines (95% CI) for domestic (blue dots) and wild (green diamonds) ecotopes. Fitted GLS-MLPE model in Eq 1. B, geographic distribution of the 25 collection sites across Loja province (elevation map) used for estimating *R. ecuadoriensis* gene flow with geographic distance. Collection sites ID labels: EX, La Extensa; SJ, San Jacinto; HY, EL Huayco; RT, Santa Rita; NJ, Naranjillo; GL, Galapagos; SS, Santa Rosa; TR, Tuburo; YS, Camayos; NT, San Antonio de Taparuca; AZ, Ardanza; GA, Guara; CQ, Chaquizhca; BM, Bella Maria; CE, Coamine; VC, Vega del Carmen; TM, Tamarindo; HG, Higida; ND, Naranjo Dulce; TC, Tacoranga; AH, Ashimingo; LM, Limones; BR, Bramaderos; CG, La Cienega; SF, San Francisco (SF). Source map: www.usgs.gov/centers/eros/science/usgs-eros-archive-digital-elevation-global-multi-resolution-terrain-elevation.

<https://doi.org/10.1371/journal.pgen.1010019.g004>

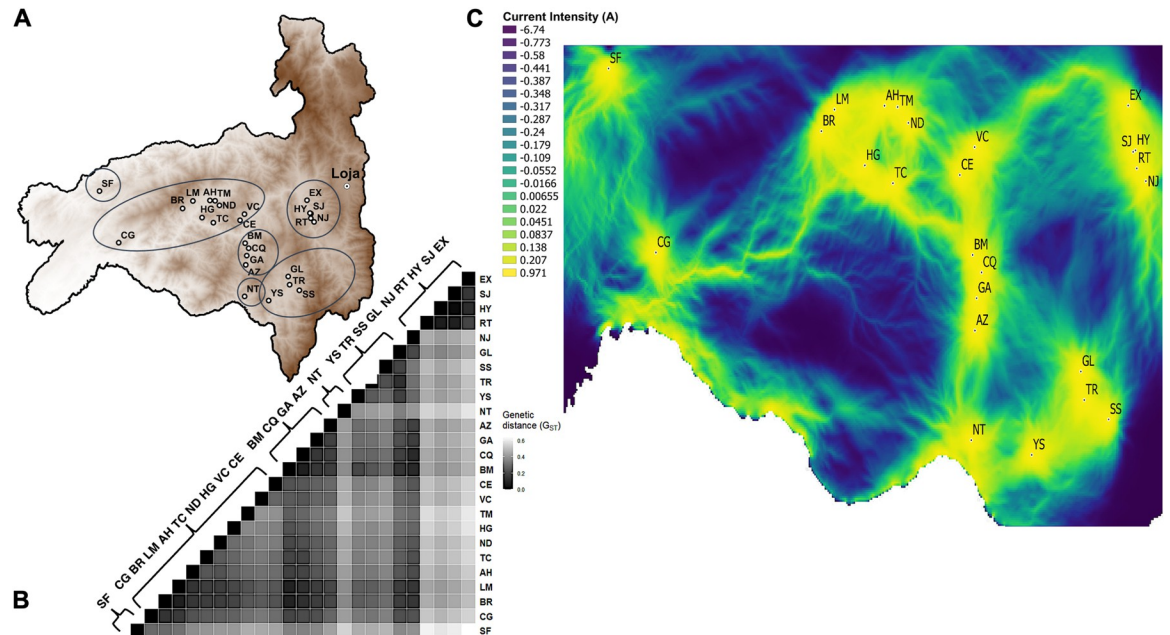


Fig 5. Landscape connectivity of *Rhodnius ecuadoriensis* in Loja province, Ecuador. A, Elevation map of the geographic location of collection sites across Loja. B, Heatmap shows pairwise genetic distances (G_{ST}) with collection sites ID labels on the right. Clusters and highly differentiated collection sites are circled in A. Grey scale indicate genetic distance with lighter colours showing higher differentiation. C, Electrical current map of Loja built from the optimised elevation surface model showing a gradient of high (yellow/light shade), medium (light greens) and low (blue/dark shade) functional connectivity across Loja. Clusters of highly connected sites are evident but isolated sites are also present across regions in Loja. Connectivity within and among clusters and collection sites is highly influenced by the landscape, specifically elevation surface. Source map: www.usgs.gov/centers/eros/science/usgs-eros-archive-digital-elevation-global-multi-resolution-terrain-elevation.

<https://doi.org/10.1371/journal.pgen.1010019.g005>

Table 1. Model selection results for the generalised mixed-effects models optimised on genetic distance (Hedrick's GST) for *R. ecuadoriensis*. The most strongly supported resistance surface model is presented first. For each resistance surface model, number of parameters plus the intercept (k), additional parameters corrected Akaike information criterion (AIC_c), delta AIC_c and AIC_c weight (ω) are provided.

Resistance surface model	Type	k	AIC_c	Delta AIC_c	ω
Elevation	single	4	-749.51	0	0.76
Distance	single	2	-747.25	2.26	0.24
Roads	single	6	-736.25	13.26	0.0010
Elevation + Roads	composite	9	-729.55	19.96	3.49e-05
Land	Single	12	-720.26	29.25	3.35e-07
Elevation + Land cover	composite	15	-687.82	61.70	3.03e-14
Land cover + Roads	composite	17	-648.63	100.88	9.37e-23
Null model	single	1	-565.08	184.43	6.75e-41
Elevation + Land cover + Roads	composite	20	-520.44	229.08	1.36e-50

<https://doi.org/10.1371/journal.pgen.1010019.t001>

both high and low genetic differentiation among collection sites (Fig 5A and 5B). San Francisco (SF) and San Antonio (NT) were two examples of clear, and mutually distinct, outliers in genetic terms. Santa Rita (RT), El Huayco (HY), San Jacinto (SJ) and La Extensa (EX) were genetically and geographically close but highly differentiated from the rest. Overall, some clusters of collection sites were evident as well as instances differentiation within and among clusters (S5 Table).

The pattern of population genomic differentiation was iteratively regressed with different combinations of landscape variables and parameters using the ResistanceGA [69] optimisation framework (see Methods). The optimisation process involves estimating unbiased resistance values for a given combination of surfaces and selecting the best (true) model representing the genomic pattern. To rule out collinearity between landscape variables, we calculated Spearman's correlation coefficient, ρ , between all pairs of surfaces which resulted in small and/or negative ($\rho < 0.29$) correlations (S6 Table). Similarly, a scatterplot matrix did not show highly correlated surfaces (S3 Fig).

Our three ResistanceGA optimisation replicates (see Methods) showed comparable results. In all replicates, the single elevation surface showed the lowest AIC_c values and the highest AIC_c weight compared to the other single and composite optimised surfaces (Table 1 is a replicate example). Delta AIC_c shows the AIC_c difference between the elevation surface (best model) and the rest of the (combination of) surfaces. A difference of ~ 2.26 units between elevation surface and a distance-only model was evident which suggests elevation surface is a better predictor than geographic distance, although geographic distance remains a strong predictor. Optimisation of the elevation surface parameters confirmed that gene flow resistance increases with altitude up to the highest resistance at approximately 2,400 m.a.s.l. (S4 Fig).

To evaluate the robustness of our optimisation procedure and test the effect of uneven distribution of sample sites, we ran a bootstrap analysis with resampling of the sites at each iteration. Interestingly, the bootstrap analysis revealed that, when resampling 85% of the collection sites, the optimised elevation surface model was ranked the top model in only 43.2% of the bootstrap iterations compared to 46% of the times in which a distance-only model was better (Table 2). The fact that elevation surface was slightly less supported in the bootstrap analysis is likely due to the irregular distribution of sites across the study area and altitudes [70].

To assist with the identification of vector management zones for regional health authorities, an electrical current map was built by applying a circuit theory algorithm [71,72] on the optimised elevation surface model (Fig 5C). Specifically, the algorithm simulates the passing of an

Table 2. Summary of bootstrap analysis. For each resistance surface model, number of parameters plus the intercept (k), and average (Avg) additional parameters corrected Akaike information criterion (AIC_c), AIC_c weight (ω), rank, and frequency the model was top ranked are provided.

Resistance surface model	k	Avg AIC	Avg AIC_c	ω	Avg rank	Top model (%)
Elevation	4	-535.59	-533.09	0.40	1.62	43.2
Distance	2	-531.44	-530.78	0.60	2.33	46
Land cover	12	-526.59	-487.59	4.17e-05	3.91	10.8
Roads	6	-523.81	-517.81	0.0008	4.18	0
Elevation + Roads	9	-525.76	-509.40	2.80e-06	4.40	0
Elevation + Land cover	15	-521.94	-425.94	1.45e-21	5.29	0
Land cover + Roads	17	-516.51	-312.51	3.97e-46	6.59	0
Elevation + Land cover + Roads	20	-511.14	328.86	1.11e-185	7.68	0

<https://doi.org/10.1371/journal.pgen.1010019.t002>

electric current across grids (zones) with low/high optimised resistance values. Low resistance grids are highlighted as high current intensity zones (yellow/light zones in Fig 5C) in which high population connectivity, and therefore high degree of gene flow, is predicted. The map showed different gradients of connectivity within and among western, central, eastern and southern Loja province. These included individually isolated populations (e.g. SF & CG), isolated clusters (e.g. EX; SJ; HY; RT; NJ); as well as well-connected hubs (e.g., BR-LM, AH-TM-ND, HG-TC and CE-VC).

Discussion

In this study we make several core observations: *R. ecuadoriensis* do invade houses from wild populations, *R. ecuadoriensis* loci associated with the domestic niche can be identified within our limited marker set and mapped to annotated triatomine genomic regions, and the landscape drivers of vector dispersal can be identified. Consistent with frequent house invasion, high levels of gene flow between multiple domestic and wild *R. ecuadoriensis* populations were detected by hierarchical analysis. Low and largely non-significant pairwise F_{ST} values, as well as interleaved sample clustering based on phylogenetic and discriminant analyses were also consistent with house invasion. Significantly elevated allelic richness in wild sites by comparison to nearby domestic foci clearly confirmed that dispersal occurred most frequently from wild ecotopes into domestic structures. Genome scans across these parallel events of colonisation to the domestic niche revealed possible evidence of ‘adaptation with geneflow’, with key outlier loci associated with colonisation of built domestic structures and, presumably, human blood feeding—several of which mapped to the *R. prolixus* genome. A strong signature of isolation-by-distance (IBD) was observable throughout the dataset, an effect less pronounced between domestic sites than between wild foci. Formal landscape genomic analyses revealed elevation surface as the major barrier to genetic connectivity between populations. Landscape genomic analysis enabled a spatial model of vector connectivity to be elaborated, informing ongoing control efforts in the region and providing a model for mapping the dispersal potential of triatomines and other disease vectors.

Vector control is the mainstay of Chagas Disease control [11]. Widespread wild reservoir hosts, as well as a lack of safe treatment options [73,74] and associated healthcare infrastructure, mean that transmission cannot be blocked by reducing parasite prevalence in human and animal hosts [75]. Our data indicate that elimination of domesticated *R. ecuadoriensis* in Ecuador will be frustrated by repeated re-invasion from the wild environment. Similar risks to effective control are posed by wild *T. infestans* in the southern cone region [12], *R. prolixus* in Los Llanos of Colombia and Venezuela [13] and potentially elsewhere in Latin America where

competent vectors are present in the wild environment and nearby domestic locales (e.g., *T. sordida*, *T. maculata*, *R. pallelescens* and others [14,15]).

Understanding evolutionary processes that underpin the colonisation of the domestic environment by arthropod vectors, and their specialisation to feeding on humans, is required to characterize their vectorial capacity. Hybrid ancestry in *Culex pipiens*, for example, is thought to contribute to the biting preference for humans [3]. Human feeding preference can be rapidly genetically selected for in *Anopheles gambiae* [76]. Specialisation of *Aedes aegypti* on humans, and resultant global outbreaks of dengue, yellow fever, and Chikungunya viruses, may be traceable to SNPs associated with the emergence of differential ligand-sensitivity of the odorant receptor *AaegOr4* in East Africa [2]. In triatomines, the nature of genetic adaptations that have enabled the widespread dispersal of successful lineages are far from clear. *T. infestans*, thought to have originated in the Western Andean region of Bolivia, spread rapidly among human dwellings in the Southern Cone region of South America before its near eradication in the 1990s [10]. Cytogenetic analyses suggest this early expansion was accompanied by a substantial reduction in genome size [77], but the significance of such a change is not clear. The advantage of the *R. ecuadoriensis* system we describe is that it may be able to capture multiple parallel adaptive processes and; therefore, can assist in the identification of common evolutionary features associated with colonisation of the domestic environment. Despite limited genomic coverage, and with no *R. ecuadoriensis* reference genome available, we mapped outlier loci to genes in the *R. prolixus* draft genome, and found hits related to salivary enzyme production [65], as well as embryonic development [63]. However, these findings represent only a small first step towards understanding domestic adaptation in triatomines. Our methodological pathway was limited to comparing allele frequencies at a relatively small fraction of genomic loci between triatomine natural populations in order to identify outlier loci associated with a given niche, and map them to genomic regions in *R. prolixus* ([30,78]). Although, these genes may have a role in domestic adaptation in triatomines, genome-wide association studies, quantitative trait locus mapping or CRISPR/Cas9 gene knockout approaches are necessary to fully reveal the genomic architecture of adaptation to the domestic setting. Nevertheless, these findings motivate us to investigate further putative genes involved in local adaptation to the domestic environment such as blood-feeding [79], sensory cues and host-seeking behaviour [28,80], as well as human blood detoxification [79,81]. Recent data from our group in Loja province shows that, without doubt, domestic *R. ecuadoriensis* feed extensively on human blood [82]. To adequately explore the genomic bases of adaptive traits in triatomines, future work should focus not only on improving functional annotation of triatomine genomes, but also robust experimental designs (e.g., common-garden or reciprocal transplant experiments [83,84]), to enable genotype and phenotype to be linked.

Our analyses identified a strong signal of genetic IBD among *R. ecuadoriensis* populations across our study area. Geographic partitioning at this scale is consistent with limited autonomous dispersal capabilities of triatomines which are, in the main, poor fliers [41]. Wind-blown dispersal observed in smaller vector species is unlikely in triatomines [85]. Passive dispersal of triatomine vectors alongside the movements of their human hosts, which certainly underpins the successful dispersal of other domesticated vector species, is more likely (e.g., *Aedes spp.* [86,87]). Lower IBD observed among domestic sites than wild sites may be consistent with passive dispersal alongside humans in the former. We observed a similar phenomenon among parasite isolates from the same region in a previous study [59] in which *T. cruzi* domestic/peridomicile isolates showed no spatial structure in comparison with wild isolates. Nonetheless, our formal exploration of the landscape drivers of vector dispersal did not reveal an important effect of roads, and it is not clear to what extent human dispersal of vectors takes place based on our data alone.

According to our landscape genomic analysis, elevation surface is a key predictor of connectivity/discontinuity among *R. ecuadoriensis* populations. Our machine learning (ML) optimisation procedure provides objective parameterisation of altitude resistance values to *R. ecuadoriensis* gene flow [88]. Based on our landscape model predictions we were able to construct an electric current map (Fig 5C) to assist medical entomologists and policy makers in understanding vector dispersal routes. Current vector control strategies in Loja target a single civic administrative unit (neighbourhood or town) for any given insecticidal intervention [55]. Historical vector control in Loja has been sporadic and limited insecticide spraying that varied yearly (from 2004 to 2014) to only a small number of parishes due to budgetary constraints [89]. Our data and model suggest this approach may be effective for certain communities (e.g., SF, CG, NT and YS, Fig 5). However, for highly connected hubs (e.g. BM, GA, CQ, AZ), successful longer term triatomine control (e.g., insecticide spraying, house improvement, window nets, etc.) will depend on simultaneous intervention in multiple connected communities.

In Ecuador, as with many other endemic regions in Latin America, efforts to control Chagas disease may be complicated in the long term by substantial wild populations of secondary triatomine vectors [16]. As with many other vector borne diseases, there is also a strong case for the use of integrated vector management (IVM) for Chagas disease, where improvements to housing, education, community engagement, in addition to bed net use and insecticide spraying are all likely to be necessary to achieve sustained control [55,90]. Our data clearly indicate that triatomines do invade houses in Loja and low-lying valleys provide routes for vector dispersal between communities and cost-effective IVM must be underpinned by this understanding of vector population structure. Fortunately, genomic and analytical tools can now furnish much of the detail, although better genomic resources for secondary triatomine vector species are required to reveal the process of vector adaptation to the human host. Targeting secondary vector species like *R. ecuadoriensis* must now be a priority for health authorities, as these now represent the most pernicious and persistent barrier to controlling residual Chagas disease transmission.

Methods

Sample collection and study area

Rhodnius ecuadoriensis triatomine bugs ($n = 272$; S1 Table) were derived from a larger collection in the Center for Research on Health in Latin America (CISeAL) of Pontificia Universidad Católica del Ecuador (PUCE). *Rhodnius prolixus* samples ($n = 6$) were provided by the London School of Hygiene and Tropical Medicine and sequenced as an outgroup, as well as to assist with the decontamination of the of 2b-RAD reads and their mapping to functional regions in the draft *R. prolixus* genome [27]. The CISeAL triatomine collection has been gathered since 2004 from domestic (human built environment) and wild (animals nests, burrows, etc) ecotopes during field surveys across Loja, Ecuador. Surveys have occurred throughout the year but 80% of the time during the summer, from June to August [58]. Houses and wild locations have been selected over the years by random sampling, but depending on rough terrain accessibility, resource availability and community participation [55,91,92]. Domestic *R. ecuadoriensis* were collected inside houses (e.g., rooms, underneath beds and clothing, walls, etc) using the one-hour-man method described in previous studies [16,55,91]. Wild *R. ecuadoriensis* were collected in animals (bird/squirrel/mouse) nests attached to trees and bushes surrounding domestic collection sites [54,56,92].

This study triatomine subset ($n = 272$) was composed of spatially widespread collection sites ($n = 25$) across Loja separated by 0.4 to 100 Km (Fig 4). Sites were located at different ecotopes (e.g., domestic and wild ecotopes separated by 0.1 to 3 Km—Fig 2), altitudes (up to 1542.9

m.a.s.l.—S5 Fig), vegetation types (e.g., tree/bush forest, cropland, etc.—S6 Fig) and adjacent to different road infrastructure (e.g., highways, tertiary roads, etc.—S7 Fig). As mentioned above, we defined *R. ecuadoriensis* as domestic/wild based on whether they were collected in the built environment or wild animals nests, respectively. When specimens were available we selected triatomines from different houses/wild sites within a locale to have a good representation of the site.

The triatomines were collected under Ecuadorian collection permits: N° 002–07 IC-FAU-DNBAPVS/MA; N° 003–2011-IC-FAU-DLP-MA; N° 006-IC-FAU-DLP-MA-2010; N° 010-IC-FAN-DPEO-MAE; N° 011–2015- IC-INF-VS-DPL-MA; MAE-DNB-CM-2015-0030 and internal mobilization guide N° 001–2018-UPN-VS-DPAL-MAE and N° 017–2018-UPN-VS-DPAL-MAE. All these samples were exported to the University of Glasgow by the scientific export authorization N°70–2018-EXP-CM-FAU-DNB/MA.

Genomic DNA extraction and sequencing

Genomic DNA (gDNA) was extracted in 88.2% (443/502) of the samples using a SSNT/Salt precipitation method [93] previously applied in triatomine bugs [94]. For each sample, gDNA concentration was > 25 ng/μL and 288.4 ng/UL (sd. ± 241.8) on average with purity ratios (260/280 and 260/230) of 1.87 (sd. ± 0.10) and 2.30 (sd. ± 0.97), respectively. gDNA was digested with the CspCI Type IIB restriction enzyme (IIB-REase—New England BioLabs, Inc.) which has shown to yield a high marker density in triatomine [94]. DNA fragments (36bp) were ligated to Illumina single-end adaptors and a specific barcode added during PCR amplification to construct 382 150bp 2bRAD libraries [95]. Libraries were homogenised to an approximate similar concentration, purified with magnetic beads [96] and pooled in two separate batches (n = 191). Each batch was sequenced separately on 1-flowcell (2 lanes) HiSeq 2500 (Illumina) Rapid Mode platform with a single-end (1x50 bp) setup using v2 SBS chemistry at the Science for Life Laboratory (SciLifeLab, Stockholm, Sweden), which also implemented the reads demultiplexing and their in-house quality-filtering.

Bioinformatics of 2b-RAD sequenced data

Data cleaning and decontamination. Demultiplexed raw data quality scores were verified in FastQC software v0.11.9 (<http://www.bioinformatics.babraham.ac.uk/projects/fastqc/>). 2.3% (16/689) Million reads (Mreads) were removed due to incomplete CspCI restriction site (36 bp) and having across read quality score below 30 [97]. The 624.7 high quality Mreads with integrate restriction site had their Illumina adaptors and barcodes trimmed, and reads were forwarded (5'-3') using custom scripts. To exclude non-target sequences, 1.2 Mreads (0.2%) mapping to bacteria, virus, archaeal, *Trypanosoma cruzi* [98] and *homo sapiens* (Genome Reference Consortium human build 38) genomes were removed using DeconSeq standalone v4.3 [99] with an alignment identity threshold of 85% and Kraken [100] taxonomic classifier (S1 Methods). After decontamination, each sample yielded on average 1.6 Million reads (inter-quartile range = 1.9 Mreads).

Optimisation and genotyping. As advised in refs. [101,102], we optimised STACKS v2.55 [103] DENOVO_MAP.PL programme by varying at a time one of the main controlling parameters (-m -M and -n, -N) on each run while keeping the rest of the parameters at the setting used in early experiments (e.g., -m 5, -M 2, -n 1, -N 4, -alpha 0.01, -bound_low 0, -bound_high 0.01, -r 0.8, -min_maf 0.01 [94]). These parameters control the minimum number of raw reads required to form a stack (a putative allele) which is comparable to the minimum depth of coverage (-m), the number of mismatches allowed between stacks (putative alleles) to merge them into a putative locus which is comparable to the number of nucleotide

mismatches allowed (-M), the number of mismatches allowed between stacks (putative loci) during construction of the catalog that contains all loci and alleles of the population (-n) and the number of mismatches allowed to align secondary reads (reads that did not form stacks) to assemble putative loci to increase locus depth (-N) [103]. The parameter combination yielding the highest number of SNPs with the least missing data and genotyping error rate was chosen to be the optimal set (S2 Methods). Genotypes below a quality score of 30, and samples with above 50% missing genotypes across sites and among loci were removed from downstream analysis using the VCFtools software suite v0.1.5 [104]. The remaining missing genotypes (< 0.5%) were imputed using the k-nearest neighbour genotype imputation (LDkNNi) method [105] implemented in the TASSEL software v5 [106].

Genomic differentiation between domestic and wild ecotopes

Genetic diversity and linkage disequilibrium. Genetic diversity measures (e.g., observed (H_O) and gene diversity (H_E), inbreeding coefficient (F_{IS}) and allelic richness (Ar))—S2 Table) were calculated for each collection site, and ecotopes (domestic and wild) within collection sites, in the HIERFSTAT [107] and pegas [108] packages in R [109]. Sample-size corrected Ar was calculated using the rarefaction method [62] implemented in the PopGenReport [110] R package. To evaluate the percentage of SNP markers in linkage disequilibrium (LD), correlation coefficient (r^2) estimates were calculated between markers pairs using the GUS-LD R package [111] which revealed a very low percentage (< 0.20%). To observe whether genetic diversity difference between ecotope pairs was significant, a permutation-based (10,000 permutations) two sample t-test was performed on each pair diversity values using the RVAideMemoire R package (<https://www.rdocumentation.org/packages/RVAideMemoire>).

Individual-based genomic differentiation. Genomic differentiation among *R. ecuadoriensis* domestic and wild samples within a subset of seven collection sites (Fig 2A) was visualised in a Neighbour-Joining midpoint tree [112] (Fig 2B) built from Euclidean genetic distances of allele frequencies with the ape [113] R package. Tree components were edited in FigTree software v1.4.3 (<http://tree.bio.ed.ac.uk/software/figtree/>) to better illustrate domestic and wild samples, and their overall clustering pattern. To explore samples genomic differentiation further, a DAPC [114] was performed in the same seven collection sites with the adegenet [115] R package (Fig 2C). The most likely *a priori* number of clusters was chosen based on the lowest Bayesian information criterion (BIC). In the DAPC, all principal components (PCs) and the eigenvectors of the first three DA discriminant functions were kept for visualizing the samples individual coordinates of different PCs linear combinations (S8 Fig).

Pairwise F_{ST} comparisons. To support previous hierarchical analyses, pairwise F_{ST} comparisons [67] (Fig 2D) were performed between *R. ecuadoriensis* from domestic and wild ecotopes within the seven collection sites (Fig 2A). In this study, F_{ST} was exploited as a measure of genomic connectivity (flow) between ecotopes within given collection sites. Specifically, Nei's F_{ST} [116] pairwise comparisons were computed in adegenet R package and tested at 5% significance via 999 permutations of individuals selected randomly within and between groups. P-values were corrected for multiple comparisons using the false discovery rate (FDR) method [117] in the function `p.adjust` of the stats R package [109].

Hierarchical F-statistics. *R. ecuadoriensis* molecular variation was explored at a four-level (e.g., among collection sites, among ecotopes (domestic or wild) within collection sites, among collection year within collection sites and among individuals within populations) hierarchy of population structure. For each hierarchy, a F-statistic (with 95% C.I.) was calculated, and its significance tested via 999 randomised permutations with the HIERFSTAT R package. For comparison and given not all sites had both ecotopes, two hierarchical analysis were

performed, one with the total collection sites ($n = 25$) and the other with a subset of collection sites ($n = 7$) with samples collected in both ecotopes (S3 Table).

Domestic-wild SNP association analyses

As a response of *R. ecuadoriensis* ecotopes fluxes in multiple collection sites across Loja, we screened for SNP RADseq markers under a strong signal of selection (outlier loci). The power for detecting outlier loci of four different approaches, Random Forest (RF) machine learning (ML) classification algorithm (implemented in refs. [118–120]), redundancy analysis (RDA) constraint ordination [121], and OutFlank [122] and fsthet [123] F_{ST} -outlier methods, was evaluated using a roughly similar number of domestic ($n = 56$) and wild ($n = 52$) *R. ecuadoriensis* across Loja province sharing a total of 2552 SNPs.

Random forest. The RF algorithm [124] implemented in the randomForest [125] R package was used to build a series of recursive decision trees (S3 Methods), or forest, to classify domestic and wild *R. ecuadoriensis* based on their shared SNPs (predictors) covarying to a specific ecotope (response variable). Within each RF run, decision trees were trained by random subsampling with replacement 66.6% of triatomine samples (training dataset), for which aleatory selected SNPs were top-ranked classifiers when minimizing the most within-ecotope variation (that is, partitioning triatomine by ecotope). Trained trees predictive power was tested with the remaining 33.3% triatomine samples ('Out-of-bag' test dataset) in which ecotope misclassification of samples estimated an OOB-ER for that RF run; SNPs importance classification accuracy was averaged among the total number of trees created in a given RF. Three independent (spatial structure-corrected) RFs with 100,000 trees were run and their convergence on SNPs importance classification accuracy was evaluated by Pearson's correlation test. Top-ranked SNPs (Fig 3A inset) among the three RFs (that is, importance classification accuracy above 3) were chosen for backwards purging, as implemented in refs. [119,126]. Backwards purging (Fig 3A) iteratively runs RFs starting with the full top-ranked SNPs and discarding the least important ones before the next iteration until only two were left. The subset with the lowest OOB-ER contained SNPs outlying strongly for the ecotope response.

Redundancy analysis. Outlier loci likely under selection were also identified using RDA multivariate constrained ordination [127] implemented in the vegan [128,129] R package. First, a matrix fitted values were obtained using multivariate linear regression between a matrix of genotypes (response) and ecotopes (explanatory) with an additional term controlling for spatial structure (based on the three first axes of an individual principal coordinates of each sample). Then, principal component analysis (PCA) on the fitted values matrix resulted in a constrained axis composed from the variation explained, 'redundancy', by our explanatory variable. Overall RDA model and variation explained by the constrained RDA axis were tested for significance via 999 permutations designed for constrained correspondence analysis. Additionally, SNPs (Fig 3B) and samples (Fig 3C) coordinates were scaled and plotted in the ordination space to see their relationship with the constrained axis (RDA 1), ecotope. SNPs z-transformed loadings separated by ± 2 and ± 3 standard deviations (permissible and conservative thresholds, respectively) from the mean distribution of the total SNPs loadings in our RDA axis were considered under selection (Fig 3B) (for further details on step-by-step RDA see S3 Methods and refs. [121,130,131]).

F_{ST} -Heterozygosity outlier method. The F_{ST} -Heterozygosity outlier method aims to identify loci with strong allele differences among ecotopes. First, ecotope differentiation for each locus is calculated using Wright's F_{ST} without sample correction. The distribution of these values is expected to have a chi-squared shape. The main goal is inferring a null F_{ST} distribution from neutral loci not strongly affected by diversifying selection [122]. Therefore, a best-fit to the chi-squared F_{ST} distribution was achieved by trimming the lowest and highest

F_{ST} values (loci in the tails of the distribution are likely to be under effective diversifying selection) and considering only the values in the centre (neutral loci and loci experiencing spatial uniform balancing selection). Loci with unusual F_{ST} values relative to this fitted distribution can be thought of experiencing additional diversifying selection [122,123]. We used two R packages to accomplish this analysis, OutFlank [122] (Fig 3D left) and fsthet [123] (Fig 3D right), and compared the results. The difference between the packages is that fsthet uses smoothed quantiles of the empirical F_{ST} -Heterozygosity distribution to identify outlier loci and does not assume a particular distribution or model of evolution as compared to OutFlank. We set OutFlank function with proportion of lower and upper loci trimmed to 0.06 and 0.35, respectively, and the rest of the values to default.

Mapping SNP outlier loci. In order to identify genes that may be responsible for local adaptation in the Chagas disease vector, *R. ecuadoriensis*, to the domestic environment we mapped the SNPs found in the association analyses to the *R. prolixus* annotated genome [27]. We used the BWA alignment tool implemented in DeconSeq software v0.4.3 [99] to map SNPs sequences (38 bp) at a minimum alignment threshold of 85. The sequences of the regions (60-300kb) in which our SNPs aligned were BLAST searched and compared to the *R. prolixus* genome.

Estimating gene flow with distance. Matrices of genetic (F_{ST} [116]) and geographic (Km) distances (Fig 4A) between the 25 collection sites (Fig 4B), and between domestic and wild collection sites separately, were obtained with the adegenet and raster [132] R packages, respectively. Mantel tests [133] were performed on those matrices using the ecodist [134] R packages. Genetic and geographic correlation between domestic and wild ecotopes was also viewed separately by fitting a generalised least square (GLS) model with a maximum likelihood population effects correction (MLPE) [135] implemented in the corMLPE (<https://github.com/nspope/corMLPE/>) R package and assuming a linear relationship

$$Y_{ij} = \alpha + \beta(X_{ij} - \bar{x}) + H_i + \tau_{ij} + e_{ij} \quad (\text{Eq1})$$

between two distance matrices based on genetic and geographic distance measures, Y and X, respectively. Centring the X_{ij} in about its mean, \bar{x} , removes the correlation between the estimates of α and β [135]. H_i , determines the ecotope and the τ_{ij} term adds the MLPE random effect correlation structure.

Estimating gene flow with resistance

Genetic distances. Given genomic differentiation between domestic and wild ecotopes was low, we combined all samples within a collection site and used collection site as the unit in our landscape genetic analysis. Collection site units are logistically and budgetary important when carrying out triatomine surveys and insecticide spraying. Hierarchical, phylogenetic and DAPC analyses also suggested *R. ecuadoriensis* samples were closely clustered by collection sites. To estimate ancestry of individuals at each collection site and support our clustering criteria, an ADMIXTURE [136] analysis was performed using a 5-step expectation-maximization algorithm and 10-fold cross-validation with 200 bootstrap resampling iterations to estimate the standard errors for $K = 2-30$ (S1 and S2 Figs). Using a landscape genomics mixed modelling framework (Fig 1), we aimed to disentangle the effects of landscape heterogeneity on *R. ecuadoriensis* population structure and gene flow (S4 Methods). A Hedrick's G_{ST} [66], which corrects for sampling limited populations [137], distance matrix among the 25 collection sites (Fig 5B) was obtained in the GenoDive v3.04 [138] software (S5 Table). In addition, we ran a Pearson's correlation test between the Hedrick's G_{ST} matrix, and Meriman's standardised F_{ST} [68] and F_{ST} [67] matrices, calculated in the same software, to evaluate the consistency of genomic differentiation pattern among collection sites with different genetic distance measures.

GIS data collection and preparation. Elevation, land cover and road network (hereafter, surfaces—S5, S6 and S7 Figs) landscape variables were chosen over temperature and precipitation to test *R. ecuadoriensis* dispersal and gene flow and to avoid multicollinearity and overfitting in our landscape mixed models. For the continuous surface (elevation surface—S5 Fig), only monomolecular transformations (e.g., S4 Fig) with any possible shape and maximum parameters were used to explore the relationship between gene flow and altitude. Our categorical surfaces, land cover and road network, were reclassified as follows. Those highly fragmented land cover categories (e.g., cultivated and managed areas) were reclassified to the least resistance of gene flow, whereas regular flooded areas and water bodies were reclassified to the highest resistance values (S6 Fig and S7 and S8 Tables). High transitable roads (e.g., highways and tertiary roads) were assigned to the least resistant values, whereas absence of roads were assigned to the highest resistance values (S9 Table). Original GIS surfaces were obtained from multiple sources (S10 Table) and transformed to have the same format (raster), resolution (250 m² grid), extent (~ 97 Km²) and coordinate reference system (Universal Transverse Mercator (UTM)). Spearman's rank correlation coefficient (ρ) tests were run (S6 Table) and plotted (S3 Fig) on each pair of surfaces to ensure variables were uncorrelated ($\rho < 0.29$ based on Cohen [139]). All three surfaces original values were transformed to the same scale (i.e., a minimum value of 1 and a maximum of 100) to meet our initial hypothesis.

ResistanceGA principle. The genetic algorithm [140] implemented in the R package, ResistanceGA [69], was used for multiple and single-surface optimization of resistance values to gene flow in the above surfaces (S4 Methods). The method works by correlating genomic (response) and effective (predictor) distances (derived from a random-walk commute time algorithm [141]—S4 Methods) matrices through a maximum likelihood population effects [135] model and, on each iteration, evaluates the best resistance parameters based on a ML objective function, log-likelihood in our case. Simulating the process of evolution on each iteration, the best model and parameters are selected and passed over the next generation with some random change on parameter values to explore the parameter space widely.

Multiple surface optimisation. We performed three replicate runs to optimise all possible combinations of our surfaces (hereafter, composite surfaces), including surfaces individually (hereafter, single surfaces) to generate models with optimised resistance values. The major GA algorithm options were set to default, except for the 'pop.mult' which was set to 20 to increase the number of parameters to evaluate on each surface every iteration. All optimisation processes were run in parallel with 10–20 cores in a Debian cluster (<http://userweb.eng.gla.ac.uk/umer.ijaz/#orion>) at the University of Glasgow. Running times varied from days to weeks depending on surface size and number combined at a time.

Model selection. Composite and single surface models, including an intercept-only (null model) and a geographic distance (resistance grid cells are set to 1 to model isolation-by-distance) model were evaluated (Table 1) and the best model was selected based on the lowest AIC_c, AIC_c weight and Delta AIC_c. To confirm the robustness of the optimisation surfaces and controlling for potential bias due to uneven distribution of sample locations in the landscape, we carried out bootstrap resampling (10,000 iterations) in 85% of our sample locations and then fit the subset to each of the effective distance matrices from the optimised surfaces. After the bootstrapping analysis, the average AIC_c among all iterations and the percentage a model was top over all iterations was used as a criterion to rank the best model (Table 2).

Landscape connectivity model. We used the best optimised single (elevation surface) resistance surface models to estimate landscape connectivity through a circuit theory algorithm [71,72] (Fig 5C) implemented in the software CIRCUITSCAPE v5 [142]. Here, our resistance surfaces were converted into electric networks in which each grid cell represented a node connected to their neighbours by resistors of different weight. Resistor weights were

calculated from the average resistance values (i.e., optimised resistance values) of the two grid cells being connected. The algorithm applies a simulated electric current between all pairs of focal nodes (collection sites) in the network to estimate effective distances between them (S4 Methods). A current density map (Fig 5C) was obtained from those resistance distance estimations representing a random walk probability of movement through our study area.

Supporting information

S1 Methods. Data decontamination in *Rhodnius ecuadoriensis* sequenced reads.

(PDF)

S2 Methods. Optimisation of genotyping strategy.

(PDF)

S3 Methods. Genomic scans in domestic and wild *Rhodnius ecuadoriensis*.

(PDF)

S4 Methods. Landscape genomics mixed modelling framework on arthropod vectors.

(PDF)

S1 Fig. Admixture bar plot of triatomine ancestries in Loja assuming $K = 20$ ancestral populations.

(PDF)

S2 Fig. Admixture analysis cross-validation error plot.

(PDF)

S3 Fig. Scatterplot matrix showing the relation between raster surfaces.

(PDF)

S4 Fig. Comparison between original and optimised relief resistance surfaces.

(PDF)

S5 Fig. Relief of Loja, Ecuador.

(PDF)

S6 Fig. Map of the land cover types present in Loja, Ecuador.

(PDF)

S7 Fig. Map of the road network of Loja, Ecuador.

(PDF)

S8 Fig. Discriminant analysis of principal components (DAPC) scatter plots of all possible PCs axes combinations comparing ecotope vs collection site in 89 samples using 2,552 SNP markers.

(PDF)

S1 Table. *Rhodnius ecuadoriensis* and *Rhodnius prolixus* (out group) samples processed in this study.

(PDF)

S2 Table. *Rhodnius ecuadoriensis* population genetic summary statistics.

(PDF)

S3 Table. Summarised results of hierarchical differentiation of molecular variance components in 2552 SNP loci on the complete ($n = 272$ samples) and a small ($n = 89$ samples)

datasets.

(PDF)

S4 Table. GLS-MLPE model results.

(PDF)

S5 Table. Matirx of pairwise G_{ST} values for the 25 collection sites in Loja.

(PDF)

S6 Table. Spearman correlation test, rho, between raster surfaces previous to optimization with ResistanceGA.

(PDF)

S7 Table. Global Land Cover 2000 project Legend.

(PDF)

S8 Table. Land cover reclassified values.

(PDF)

S9 Table. Roads reclassified values.

(PDF)

S10 Table. Original GIS data, description and collection source.

(PDF)

Acknowledgments

We thank Dr P. Johnson for advice in statistical analyses, Prof W. Peterman for helpful advice on ResistanceGA analysis, the entomological team at CISEAL for sample collection and M. Babbucci for proving custom scripts for 2b-RAD raw data cleaning. We also thank Prof D. Haydon, Prof S. Babayan and Dr R. Biek for their feedback. We thank S. Morrow for proof-reading the manuscript.

Author Contributions

Conceptualization: Luis E. Hernandez-Castro, Erin L. Landguth, Martin S. Llewellyn, Mario J. Grijalva.

Data curation: Luis E. Hernandez-Castro, Sofía Ocaña-Mayorga, Cesar A. Yumiseva, Antonella Bacigalupo, Björn Andersson.

Formal analysis: Luis E. Hernandez-Castro, Arne Jacobs, Bachar Cheaib, Casey C. Day, Erin L. Landguth.

Funding acquisition: Luis E. Hernandez-Castro, Björn Andersson, Erin L. Landguth, Martin S. Llewellyn, Mario J. Grijalva.

Investigation: Luis E. Hernandez-Castro, Arne Jacobs, Erin L. Landguth, Jaime A. Costales, Martin S. Llewellyn, Mario J. Grijalva.

Methodology: Luis E. Hernandez-Castro, Arne Jacobs, Bachar Cheaib, Casey C. Day, Björn Andersson, Louise Matthews, Erin L. Landguth, Jaime A. Costales, Martin S. Llewellyn, Mario J. Grijalva.

Project administration: Luis E. Hernandez-Castro, Anita G. Villacís, Jaime A. Costales, Martin S. Llewellyn, Mario J. Grijalva.

Resources: Anita G. Villacís, Bachar Cheaib, Sofía Ocaña-Mayorga, Cesar A. Yumiseva, Antonella Bacigalupo, Björn Andersson, Louise Matthews, Jaime A. Costales, Martin S. Llewellyn, Mario J. Grijalva.

Supervision: Luis E. Hernandez-Castro, Arne Jacobs, Casey C. Day, Louise Matthews, Erin L. Landguth, Martin S. Llewellyn, Mario J. Grijalva.

Visualization: Luis E. Hernandez-Castro, Arne Jacobs, Casey C. Day, Erin L. Landguth.

Writing – original draft: Luis E. Hernandez-Castro, Martin S. Llewellyn.

Writing – review & editing: Anita G. Villacís, Arne Jacobs, Bachar Cheaib, Casey C. Day, Sofía Ocaña-Mayorga, Cesar A. Yumiseva, Antonella Bacigalupo, Björn Andersson, Louise Matthews, Erin L. Landguth, Jaime A. Costales, Mario J. Grijalva.

References

1. Powell JR, Tabachnick WJ. History of domestication and spread of *Aedes aegypti*—a review. Memórias do Instituto Oswaldo Cruz. Instituto Oswaldo Cruz; 2013. pp. 11–17. <https://doi.org/10.1590/0074-0276130395> PMID: 24473798
2. McBride CS, Baier F, Omondi AB, Spitzer SA, Lutomiah J, Sang R, et al. Evolution of mosquito preference for humans linked to an odorant receptor. Nature. 2014; 515: 222–227. <https://doi.org/10.1038/nature13964> PMID: 25391959
3. Kilpatrick AM, Kramer LD, Jones MJ, Marra PP, Daszak P, Fonseca DM. Genetic Influences on Mosquito Feeding Behavior and the Emergence of Zoonotic Pathogens. Am J Trop Med Hyg. 2007; 77: 667–671. <https://doi.org/10.4269/ajtmh.2007.77.667> PMID: 17978068
4. Fritz ML, Walker ED, Miller JR, Severson DW, Dworkin I. Divergent host preferences of above- and below-ground *Culex pipiens* mosquitoes and their hybrid offspring. Med Vet Entomol. 2015; 29: 115–123. <https://doi.org/10.1111/mve.12096> PMID: 25600086
5. Main BJ, Lee Y, Ferguson HM, Kreppel KS, Kihonda A, Govella NJ, et al. The Genetic Basis of Host Preference and Resting Behavior in the Major African Malaria Vector, *Anopheles arabiensis*. PLOS Genet. 2016; 12: e1006303. <https://doi.org/10.1371/journal.pgen.1006303> PMID: 27631375
6. Leftwich PT, Bolton M, Chapman T. Evolutionary biology and genetic techniques for insect control. Evolutionary Applications. Wiley-Blackwell; 2016. pp. 212–230. <https://doi.org/10.1111/eva.12280> PMID: 27087849
7. Powell JR. An Evolutionary Perspective on Vector-Borne Diseases. Front Genet. 2019; 10: 1266. <https://doi.org/10.3389/fgene.2019.01266> PMID: 31921304
8. WHO. WHO Chagas disease (American trypanosomiasis). 2021. Available: [https://www.who.int/news-room/fact-sheets/detail/chagas-disease-\(american-trypanosomiasis\)](https://www.who.int/news-room/fact-sheets/detail/chagas-disease-(american-trypanosomiasis))
9. Otálora-Luna F, Pérez-Sánchez AJ, Sandoval C, Aldana E. Evolution of hematophagous habit in Triatominae (Heteroptera: Reduviidae). Rev Chil Hist Nat. 2015; 88: 1–13. <https://doi.org/10.1186/S40693-014-0032-0/TABLES/2>
10. Schofield CJ, Dias JC. The Southern Cone Initiative against Chagas disease. Adv Parasitol. 1999; 42: 1–27. [https://doi.org/10.1016/s0065-308x\(08\)60147-5](https://doi.org/10.1016/s0065-308x(08)60147-5) PMID: 10050271
11. Hashimoto K, Schofield CJ. Elimination of *Rhodnius prolixus* in Central America. Parasit Vectors. 2012; 5: 45. <https://doi.org/10.1186/1756-3305-5-45> PMID: 22357219
12. Ceballos LA, Piccinali R V., Marcet PL, Vazquez-Prokopec GM, Cardinal MV, Schachter-Broide J, et al. Hidden Sylvatic Foci of the Main Vector of Chagas Disease *Triatoma infestans*: Threats to the Vector Elimination Campaign? Huete-Pérez JA, editor. PLoS Negl Trop Dis. 2011; 5: e1365. <https://doi.org/10.1371/journal.pntd.0001365> PMID: 22039559
13. Fitzpatrick S, Feliciangeli MD, Sanchez-Martin MJ, Monteiro FA, Miles MA. Molecular genetics reveal that silvatic *Rhodnius prolixus* do colonise rural houses. PLoS Negl Trop Dis. 2008; 2: e210. <https://doi.org/10.1371/journal.pntd.0000210> PMID: 18382605
14. Rodríguez-Planes LI, Gaspe MS, Enriquez GF, Gürtler RE. Habitat-Specific Occupancy and a Meta-population Model of *Triatoma sordida* (Hemiptera: Reduviidae), a Secondary Vector of Chagas Disease, in Northeastern Argentina. J Med Entomol. 2018; 55: 370–381. <https://doi.org/10.1093/jme/tjx227> PMID: 29272421
15. Cantillo-Barraza O, Chaverra D, Marcet P, Arboleda-Sánchez S, Triana-Chávez O. *Trypanosoma cruzi* transmission in a Colombian Caribbean region suggests that secondary vectors play an

- important epidemiological role. *Parasites and Vectors*. 2014; 7. <https://doi.org/10.1186/1756-3305-7-381> PMID: 25141852
16. Grijalva MJ, Villacís AG, Ocaña-Mayorga S, Yumiseva CA, Baus EG. Limitations of selective deltamethrin application for triatomine control in central coastal Ecuador. *Parasites and Vectors*. 2011; 4: 20. <https://doi.org/10.1186/1756-3305-4-20> PMID: 21332985
 17. Villacís AG, Bustillos JJ, Depickère S, Sánchez D, Yumiseva CA, Troya-Zuleta A, et al. Would tropical climatic variations impact the genetic variability of triatomines: *Rhodnius ecuadoriensis*, principal vector of Chagas disease in Ecuador? *Acta Trop*. 2020; 209: 105530. <https://doi.org/10.1016/j.actatropica.2020.105530> PMID: 32439318
 18. Dumonteil E, Gourbiere S, Barrera-Perez M, Rodriguez-Felix E, Ruiz-Pina H, Banos-Lopez O, et al. Geographic distribution of *Triatoma dimidiata* and transmission dynamics of *Trypanosoma cruzi* in the Yucatan peninsula of Mexico. *Am J Trop Med Hyg*. 2002; 67: 176–183. Available: <http://www.ajtmh.org/content/67/2/176.short> <https://doi.org/10.4269/ajtmh.2002.67.176> PMID: 12389944
 19. Brito RN, Gorla DE, Diotaiuti L, Gomes ACF, Souza RCM, Abad-Franch F. Drivers of house invasion by sylvatic Chagas disease vectors in the Amazon-Cerrado transition: A multi-year, state-wide assessment of municipality-aggregated surveillance data. Dumonteil E, editor. *PLoS Negl Trop Dis*. 2017; 11: e0006035. <https://doi.org/10.1371/journal.pntd.0006035> PMID: 29145405
 20. Brown JE, McBride CS, Johnson P, Ritchie S, Paupy C, Bossin H, et al. Worldwide patterns of genetic differentiation imply multiple ‘domestications’ of *Aedes aegypti*, a major vector of human diseases. *Proc R Soc B Biol Sci*. 2011; 278: 2446–2454. <https://doi.org/10.1098/rspb.2010.2469> PMID: 21227970
 21. Powell JR, Gloria-Soria A, Kotsakiozi P. Recent history of *Aedes aegypti*: Vector genomics and epidemiology records. *BioScience*. Oxford University Press; 2018. pp. 854–860. <https://doi.org/10.1093/biosci/biy119> PMID: 30464351
 22. Soria-Carrasco V, Gompert Z, Comeault AA, Farkas TE, Parchman TL, Johnston JS, et al. Stick insect genomes reveal natural selection’s role in parallel speciation. *Science* (80-). 2014; 344: 738–742. <https://doi.org/10.1126/science.1252136> PMID: 24833390
 23. Zumaya-Estrada FA, Messenger LA, Lopez-Ordóñez T, Lewis MD, Flores-Lopez CA, Martínez-Ibarra AJ, et al. North American import? Charting the origins of an enigmatic *Trypanosoma cruzi* domestic genotype. *Parasites and Vectors*. 2012; 5: 226. <https://doi.org/10.1186/1756-3305-5-226> PMID: 23050833
 24. Piccinali R V., Marcet PL, Noireau F, Kitron U, Gürtler RE, Dotson EM. Molecular Population Genetics and Phylogeography of the Chagas Disease Vector *Triatoma infestans* in South America. *J Med Entomol*. 2009; 46: 796–809. <https://doi.org/10.1603/033.046.0410> PMID: 19645282
 25. Calfee E, Agra MN, Palacio MA, Ramírez SR, Coop G. Selection and hybridization shaped the rapid spread of African honey bee ancestry in the americas. *PLoS Genet*. 2020; 16: e1009038. <https://doi.org/10.1371/journal.pgen.1009038> PMID: 33075065
 26. Mikheyev AS, Tin MMY, Arora J, Seeley TD. Museum samples reveal rapid evolution by wild honey bees exposed to a novel parasite. *Nat Commun*. 2015; 6: 1–8. <https://doi.org/10.1038/ncomms8991> PMID: 26246313
 27. Mesquita RD, Vionette-Amaral RJ, Lowenberger C, Rivera-Pomar R, Monteiro FA, Minx P, et al. Genome of *Rhodnius prolixus*, an insect vector of Chagas disease, reveals unique adaptations to hematophagy and parasite infection. *Proc Natl Acad Sci*. 2015; 112: 14936–14941. <https://doi.org/10.1073/pnas.1506226112> PMID: 26627243
 28. Marchant A, Mougél F, Jacquín-Joly E, Costa J, Almeida CE, Harry M. Under-Expression of Chemosensory Genes in Domiciliary Bugs of the Chagas Disease Vector *Triatoma brasiliensis*. *PLoS Negl Trop Dis*. 2016; 10: e0005067. <https://doi.org/10.1371/journal.pntd.0005067> PMID: 27792774
 29. Liu Q, Guo Y, Zhang Y, Hu W, Li Y, Zhu D, et al. A chromosomal-level genome assembly for the insect vector for Chagas disease, *Triatoma rubrofasciata*. *Gigascience*. 2019; 8. <https://doi.org/10.1093/gigascience/giz089> PMID: 31425588
 30. Tígano A, Friesen VL. Genomics of local adaptation with gene flow. *Mol Ecol*. 2016; 25: 2144–2164. <https://doi.org/10.1111/mec.13606> PMID: 26946320
 31. Ribeiro JMC, Francischetti IMB. Role of Arthropod Saliva in Blood Feeding: Sialome and Post-Sialome Perspectives*. <https://doi.org/10.1146/annurev.ento.48.06.0402102812>. 2003; 48: 73–88. PMID: 12194906
 32. Santiago PB, de Araújo CN, Charneau S, Bastos IMD, Assumpção TCF, Queiroz RML, et al. Exploring the molecular complexity of *Triatoma dimidiata* sialome. *J Proteomics*. 2018; 174: 47–60. <https://doi.org/10.1016/j.jprot.2017.12.016> PMID: 29288089

33. Sant'Anna MRV, Soares AC, Araujo RN, Gontijo NF, Pereira MH. Triatomines (Hemiptera, Reduviidae) blood intake: Physical constraints and biological adaptations. *J Insect Physiol.* 2017; 97: 20–26. <https://doi.org/10.1016/j.jinsphys.2016.08.004> PMID: 27521585
34. Pereira MH, Gontijo NF, Guarneri AA, Sant'Anna MR, Diotaiuti L. Competitive displacement in Triatominae: the *Triatoma infestans* success. *Trends Parasitol.* 2006; 22: 516–20. <https://doi.org/10.1016/j.pt.2006.08.012> PMID: 16971183
35. Dujardin JP, Steindel M, Chavez T, Machane M, Schofield CJ. Changes in the Sexual Dimorphism of Triatominae in the Transition from Natural to Artificial Habitats. *Mem Inst Oswaldo Cruz.* 1999; 94: 565–569. <https://doi.org/10.1590/s0074-02761999000400024> PMID: 10446020
36. Leyria J, Orchard I, Lange AB. What happens after a blood meal? A transcriptome analysis of the main tissues involved in egg production in *Rhodnius prolixus*, an insect vector of Chagas disease. *PLoS Negl Trop Dis.* 2020; 14: e0008516. <https://doi.org/10.1371/journal.pntd.0008516> PMID: 33057354
37. Pires HHR, Barbosa SE, Diotaiuti L. Comparative developmental and susceptibility to insecticide of Bolivian and Brazilian populations of *Triatoma infestans*. *Mem Inst Oswaldo Cruz.* 2000; 95: 883–888. <https://doi.org/10.1590/s0074-02762000000600025> PMID: 11080780
38. De Souza RDCM Barbosa SE, Sonoda IV Azeredo BVDM, Romanha AJ, Diotaiuti L. Population dynamics of *Triatoma vitticeps* (Stål, 1859) in Itanhomi, Minas Gerais, Brazil. *Mem Inst Oswaldo Cruz.* 2008; 103: 14–20. <https://doi.org/10.1590/s0074-02762008000100002> PMID: 18368232
39. Kamimura EH, Viana MC, Lilioso M, Fontes FHM, Pires-Silva D, Valença-Barbosa C, et al. Drivers of molecular and morphometric variation in *Triatoma brasiliensis* (Hemiptera: Triatominae): The resolution of geometric morphometrics for populational structuring on a microgeographical scale. *Parasites and Vectors.* 2020; 13: 455. <https://doi.org/10.1186/s13071-020-04340-7> PMID: 32894173
40. Flores-Ferrer A, Marcou O, Walecx E, Dumonteil E, Gourbière S. Evolutionary ecology of Chagas disease; what do we know and what do we need? *Evol Appl.* 2018; 11: 470–487. <https://doi.org/10.1111/eva.12582> PMID: 29636800
41. Vazquez-Prokopec GM, Ceballos LA, Kitron U, Gürtler RE. Active dispersal of natural populations of *Triatoma infestans* (Hemiptera: Reduviidae) in rural northwestern Argentina. *J Med Entomol.* 2004; 41: 614–21. <https://doi.org/10.1603/0022-2585-41.4.614> PMID: 15311452
42. Stevens L, Dorn PL, Schmidt JO, Klotz JH, Lucero D, Klotz SA. Kissing Bugs. The Vectors of Chagas. *Advances in Parasitology.* 2011. pp. 169–192. <https://doi.org/10.1016/B978-0-12-385863-4.00008-3> PMID: 21820556
43. Gourbière S, Dorn P, Triplet F, Dumonteil E. Genetics and evolution of triatomines: from phylogeny to vector control. *Heredity (Edinb).* 2012; 108: 190–202. <https://doi.org/10.1038/hdy.2011.71> PMID: 21897436
44. Bustamante DM, Monroy MC, Rodas AG, Abraham Juarez J, Malone JB. Environmental determinants of the distribution of Chagas disease vectors in south-eastern Guatemala. *Geospat Health.* 2007; 1: 199. <https://doi.org/10.4081/gh.2007.268> PMID: 18686245
45. Ramsey JM, Ordoñez R, Cruz-Celis A, Alvear AL, Chavez V, Lopez R, et al. Distribution of domestic Triatominae and stratification of Chagas Disease transmission in Oaxaca, Mexico. *Med Vet Entomol.* 2000; 14: 19–30. <https://doi.org/10.1046/j.1365-2915.2000.00214.x> PMID: 10759308
46. Parra-Henao G, Suárez-Escudero LC, González-Caro S. Potential Distribution of Chagas Disease Vectors (Hemiptera, Reduviidae, Triatominae) in Colombia, Based on Ecological Niche Modeling. *J Trop Med.* 2016; 2016. <https://doi.org/10.1155/2016/1439090> PMID: 28115946
47. Gurgel-Gonçalves R, Galvão C, Costa J, Peterson AT. Geographic Distribution of Chagas Disease Vectors in Brazil Based on Ecological Niche Modeling. *J Trop Med.* 2012; 2012: 1–15. <https://doi.org/10.1155/2012/705326> PMID: 22523500
48. Ferro C, López M, Fuya P, Lugo L, Cordovez JM, González C. Spatial Distribution of Sand Fly Vectors and Eco-Epidemiology of Cutaneous Leishmaniasis Transmission in Colombia. Carvalho LH, editor. *PLoS One.* 2015; 10: e0139391. <https://doi.org/10.1371/journal.pone.0139391> PMID: 26431546
49. Bouyer J, Lancelot R. Using genetic data to improve species distribution models. *Infect Genet Evol.* 2018; 63: 292–294. <https://doi.org/10.1016/j.meegid.2017.03.025> PMID: 28342886
50. Manel S, Holderegger R. Ten years of landscape genetics. *Trends Ecol Evol.* 2013; 28: 614–621. <https://doi.org/10.1016/j.tree.2013.05.012> PMID: 23769416
51. Vreysen MJB, Saleh K, Mramba F, Parker A, Feldmann U, Dyck VA, et al. Sterile Insects to Enhance Agricultural Development: The Case of Sustainable Tsetse Eradication on Unguja Island, Zanzibar, Using an Area-Wide Integrated Pest Management Approach. *PLoS Negl Trop Dis.* 2014; 8: e2857. <https://doi.org/10.1371/journal.pntd.0002857> PMID: 24874883

52. Schwabl P, Llewellyn MS, Landguth EL, Andersson B, Kitron U, Costales JA, et al. Prediction and Prevention of Parasitic Diseases Using a Landscape Genomics Framework. *Trends Parasitol.* 2016 [cited 22 Mar 2017]. <https://doi.org/10.1016/j.pt.2016.10.008> PMID: 27863902
53. Hemming-Schroeder E, Lo E, Salazar C, Puente S, Yan G. Landscape Genetics: A Toolbox for Studying Vector-Borne Diseases. *Front Ecol Evol.* 2018; 6: 21. <https://doi.org/10.3389/fevo.2018.00021>
54. Grijalva MJ, Terán D, Dangles O. Dynamics of sylvatic chagas disease vectors in coastal Ecuador is driven by changes in land cover. *PLoS Negl Trop Dis.* 2014; 8: e2960. <https://doi.org/10.1371/journal.pntd.0002960> PMID: 24968118
55. Grijalva MJ, Villacis AG, Ocaña-Mayorga S, Yumiseva CA, Moncayo AL, Baus EG. Comprehensive Survey of Domiciliary Triatomine Species Capable of Transmitting Chagas Disease in Southern Ecuador. Dumonteil E, editor. *PLoS Negl Trop Dis.* 2015; 9: e0004142. <https://doi.org/10.1371/journal.pntd.0004142> PMID: 26441260
56. Grijalva MJ, Suarez-Davalos V, Villacis AG, Ocaña-Mayorga S, Dangles O. Ecological factors related to the widespread distribution of sylvatic *Rhodnius ecuadoriensis* populations in southern Ecuador. *Parasit Vectors.* 2012; 5: 17. <https://doi.org/10.1186/1756-3305-5-17> PMID: 22243930
57. Villacís AG, Grijalva MJ, Catalá SS. Phenotypic Variability of *Rhodnius ecuadoriensis* Populations at the Ecuadorian Central and Southern Andean Region. *J Med Entomol.* 2010; 47: 1034–1043. <https://doi.org/10.1603/me10053> PMID: 21175051
58. Villacís AG, Marcet PL, Yumiseva CA, Dotson EM, Tibayrenc M, Brenière SF, et al. Pioneer study of population genetics of *Rhodnius ecuadoriensis* (Hemiptera: Reduviidae) from the central coast and southern Andean regions of Ecuador. *Infect Genet Evol.* 2017; 53: 116–127. <https://doi.org/10.1016/j.meegid.2017.05.019> PMID: 28546079
59. Ocaña-Mayorga S, Llewellyn MS, Costales JA, Miles MA, Grijalva MJ. Sex, Subdivision, and Domestic Dispersal of *Trypanosoma cruzi* Lineage I in Southern Ecuador. *PLoS Negl Trop Dis.* 2010; 4: e915. <https://doi.org/10.1371/journal.pntd.0000915> PMID: 21179502
60. Costales JA, Jara-Palacios MA, Llewellyn MS, Messenger LA, Ocaña-Mayorga S, Villacís AG, et al. *Trypanosoma cruzi* population dynamics in the Central Ecuadorian Coast. *Acta Trop.* 2015. <https://doi.org/10.1016/j.actatropica.2015.07.017> PMID: 26200787
61. Monteiro FA, Wesson DM, Dotson EM, Schofield CJ, Beard CB. Phylogeny and molecular taxonomy of the rhodniini derived from mitochondrial and nuclear DNA sequences. *Am J Trop Med Hyg.* 2000; 62: 460–465. <https://doi.org/10.4269/ajtmh.2000.62.460> PMID: 11220761
62. El Mousadik A, Petit RJ. High level of genetic differentiation for allelic richness among populations of the argan tree [*Argania spinosa* (L.) Skeels] endemic to Morocco. *Theor Appl Genet.* 1996; 92: 832–839. <https://doi.org/10.1007/BF00221895> PMID: 24166548
63. Lavore A, Esponda-Behrens N, Pagola L, Rivera-Pomar R. The gap gene Krüppel of *Rhodnius prolixus* is required for segmentation and for repression of the homeotic gene sex comb-reduced. *Dev Biol.* 2014; 387: 121–129. <https://doi.org/10.1016/j.ydbio.2013.12.030> PMID: 24406318
64. Lavore A, Pagola L, Esponda-Behrens N, Rivera-Pomar R. The gap gene giant of *Rhodnius prolixus* is maternally expressed and required for proper head and abdomen formation. *Dev Biol.* 2012; 361: 147–155. <https://doi.org/10.1016/j.ydbio.2011.06.038> PMID: 21763688
65. Ribeiro JM., Andersen J, Silva-Neto MA., Pham V., Garfield M., Valenzuela J. Exploring the sialome of the blood-sucking bug *Rhodnius prolixus*. *Insect Biochem Mol Biol.* 2004; 34: 61–79. <https://doi.org/10.1016/j.ibmb.2003.09.004> PMID: 14976983
66. Hedrick PW. A standardized genetic differentiation measure. *Evolution (N Y).* 2005; 59: 1633–1638. <https://doi.org/10.1111/j.0014-3820.2005.tb01814.x> PMID: 16329237
67. Weir BS, Cockerham CC. Estimating F -statistics for the analysis of population structure. *Evolution (N Y).* 1984; 38: 1358–1370. <https://doi.org/10.1111/j.1558-5646.1984.tb05657.x> PMID: 28563791
68. Meirmans PG. Using the amova framework to estimate a standardized genetic differentiation measure. *Evolution (N Y).* 2006; 60: 2399–2402. <https://doi.org/10.1111/j.0014-3820.2006.tb01874.x> PMID: 17236430
69. Peterman WE. ResistanceGA: An R package for the optimization of resistance surfaces using genetic algorithms. *Methods Ecol Evol.* 2018; 9: 1638–1647. <https://doi.org/10.1111/2041-210X.12984>
70. Dudaniec RY, Worthington Wilmer J, Hanson JO, Warren M, Bell S, Rhodes JR. Dealing with uncertainty in landscape genetic resistance models: a case of three co-occurring marsupials. *Mol Ecol.* 2016; 25: 470–486. <https://doi.org/10.1111/mec.13482> PMID: 26588177
71. McRae BH, Dickson BG, Keitt TH, Shah VB. Using circuit theory to model connectivity in ecology, evolution, and conservation. *Ecology.* 2008; 89: 2712–2724. <https://doi.org/10.1890/07-1861.1> PMID: 18959309

72. Kivimäki I, Shimbo M, Saerens M. Developments in the theory of randomized shortest paths with a comparison of graph node distances. *Phys A Stat Mech its Appl*. 2014; 393: 600–616. <https://doi.org/10.1016/j.physa.2013.09.016>
73. Paucar R, Moreno-Viguri E, Pérez-Silanes S. Challenges in Chagas Disease Drug Discovery: A Review. *Curr Med Chem*. 2016; 23: 3154–3170. <https://doi.org/10.2174/0929867323999160625124424> PMID: 27356544
74. Olivera MJ, Cucunubá ZM, Valencia-Hernández CA, Herazo R, Agreda-Rudenko D, Flórez C, et al. Risk factors for treatment interruption and severe adverse effects to benznidazole in adult patients with Chagas disease. *PLoS One*. 2017; 12. <https://doi.org/10.1371/journal.pone.0185033> PMID: 28949997
75. Sosa-Estani S. Advances and challenges in the treatment of Chagas disease—a global perspective. *Int J Infect Dis*. 2018; 73: 51. <https://doi.org/10.1016/j.ijid.2018.04.3539>
76. Gillies MT. Selection for host preference in *Anopheles gambiae*. *Nature*. 1964; 203: 852–854. <https://doi.org/10.1038/203852a0> PMID: 14204067
77. Panzera F, Ferreiro MJ, Pita S, Calleros L, Pérez R, Basmadjián Y, et al. Evolutionary and dispersal history of *Triatoma infestans*, main vector of Chagas disease, by chromosomal markers. *Infect Genet Evol*. 2014; 27: 105–113. <https://doi.org/10.1016/j.meegid.2014.07.006> PMID: 25017654
78. Tigano A, Shultz AJ, Edwards S V., Robertson GJ, Friesen VL. Outlier analyses to test for local adaptation to breeding grounds in a migratory arctic seabird. *Ecol Evol*. 2017; 7: 2370. <https://doi.org/10.1002/ece3.2819> PMID: 28405300
79. Santiago PB, De Araújo CN, Motta FN, Praça YR, Charneau S, Bastos IMD, et al. Proteases of hematophagous arthropod vectors are involved in blood-feeding, yolk formation and immunity—a review. *Parasites and Vectors*. BioMed Central Ltd.; 2017. pp. 1–20. <https://doi.org/10.1186/s13071-016-1943-1> PMID: 28049510
80. Guerenstein PG, Lazzari CR. Host-seeking: How triatomines acquire and make use of information to find blood. *Acta Trop*. 2009; 110: 148–158. <https://doi.org/10.1016/j.actatropica.2008.09.019> PMID: 18983971
81. Sterkel M, Perdomo HD, Guizzo MG, Barletta ABF, Nunes RD, Dias FA, et al. Tyrosine Detoxification Is an Essential Trait in the Life History of Blood-Feeding Arthropods. *Curr Biol*. 2016; 26: 2188–2193. <https://doi.org/10.1016/j.cub.2016.06.025> PMID: 27476595
82. Ocaña-Mayorga S, Bustillos JJ, Villacís AG, Pinto CM, Brenière SF, Grijalva MJ. Triatomine feeding profiles and *Trypanosoma cruzi* infection, implications in domestic and sylvatic transmission cycles in Ecuador. *Pathogens*. 2021; 10: 1–17. <https://doi.org/10.3390/pathogens10010042> PMID: 33430264
83. Martin RA, Chick LD, Garvin ML, Diamond SE. In a nutshell, a reciprocal transplant experiment reveals local adaptation and fitness trade-offs in response to urban evolution in an acorn-dwelling ant. *Evolution (N Y)*. 2021; 75: 876–887. <https://doi.org/10.1111/EVO.14191> PMID: 33586171
84. De Villemereuil P, Gaggiotti OE, Mouterde M, Till-Bottraud I. Common garden experiments in the genomic era: new perspectives and opportunities. *Hered* 2016 1163. 2015; 116: 249–254. <https://doi.org/10.1038/hdy.2015.93> PMID: 26486610
85. Huestis DL, Dao A, Diallo M, Sanogo ZL, Samake D, Yaro AS, et al. Windborne long-distance migration of malaria mosquitoes in the Sahel. *Nature*. Nature Publishing Group; 2019. pp. 404–408. <https://doi.org/10.1038/s41586-019-1622-4> PMID: 31578527
86. Brown JE, Evans BR, Zheng W, Obas V, Barrera-Martinez L, Egizi A, et al. Human impacts have shaped historical and recent evolution in *Aedes aegypti*, the dengue and yellow fever mosquito. *Evolution (N Y)*. 2014; 68: 514–525. <https://doi.org/10.1111/evo.12281> PMID: 24111703
87. Medley KA, Jenkins DG, Hoffman EA. Human-aided and natural dispersal drive gene flow across the range of an invasive mosquito. *Mol Ecol*. 2015; 24: 284–295. <https://doi.org/10.1111/mec.12925> PMID: 25230113
88. Peterman WE, Winiarski KJ, Moore CE, Carvalho C da S, Gilbert AL, Spear SF. A comparison of popular approaches to optimize landscape resistance surfaces. *Landsc Ecol*. 2019; 34: 2197–2208. <https://doi.org/10.1007/s10980-019-00870-3>
89. Quinde-Calderón L, Rios-Quituzaca P, Solorzano L, Dumonteil E. Ten years (2004–2014) of Chagas disease surveillance and vector control in Ecuador: successes and challenges. *Trop Med Int Heal*. 2016; 21: 84–92. <https://doi.org/10.1111/tmi.12620> PMID: 26458237
90. Castro-Arroyave D, Monroy MC, Irurita MI. Integrated vector control of Chagas disease in Guatemala: a case of social innovation in health. *Infect Dis Poverty*. 2020; 9: 25. <https://doi.org/10.1186/s40249-020-00639-w> PMID: 32284071
91. Grijalva MJ, Palomeque-Rodríguez FS, Costales JA, Davila S, Arcos-Teran L. High household infestation rates by synanthropic vectors of Chagas disease in southern Ecuador. *Journal of Medical*

- Entomology. Entomological Society of America; 2005. pp. 68–74. <https://doi.org/10.1093/jmedent/42.1.68> PMID: 15691011
92. Grijalva MJ, Villacis AG. Presence of *Rhodnius ecuadoriensis* in sylvatic habitats in the southern highlands (Loja Province) of Ecuador. *J Med Entomol*. 2009; 46: 708–11. <https://doi.org/10.1603/033.046.0339> PMID: 19496445
 93. Aljanabi SM, Martinez I. Universal and rapid salt-extraction of high quality genomic DNA for PCR-based techniques. *Nucleic Acids Res*. 1997; 25: 4692–4693. <https://doi.org/10.1093/nar/25.22.4692> PMID: 9358185
 94. Hernandez-Castro LE, Paterno M, Villacis AG, Andersson B, Costales JA, De Noia M, et al. 2b-RAD genotyping for population genomic studies of Chagas disease vectors: *Rhodnius ecuadoriensis* in Ecuador. *PLoS Negl Trop Dis*. 2017; 11: e0005710. <https://doi.org/10.1371/journal.pntd.0005710> PMID: 28723901
 95. Wang S, Meyer E, McKay JK, Matz M V. 2b-RAD: a simple and flexible method for genome-wide genotyping. *Nat Methods*. 2012; 9: 808–10. <https://doi.org/10.1038/nmeth.2023> PMID: 22609625
 96. DeAngelis MM, Wang DG, Hawkins TL. Solid-phase reversible immobilization for the isolation of PCR products. *Nucleic Acids Res*. 1995; 23: 4742–3. <https://doi.org/10.1093/nar/23.22.4742> PMID: 8524672
 97. O’Leary SJ, Puritz JB, Willis SC, Hollenbeck CM, Portnoy DS. These aren’t the loci you’e looking for: Principles of effective SNP filtering for molecular ecologists. *Mol Ecol*. 2018; 27: 3193–3206. <https://doi.org/10.1111/mec.14792> PMID: 29987880
 98. Franzén O, Ochaya S, Sherwood E, Lewis MD, Llewellyn MS, Miles MA, et al. Shotgun Sequencing Analysis of *Trypanosoma cruzi* Sylvio X10/1 and Comparison with *T. cruzi* VI CL Brener. Bates PA, editor. *PLoS Negl Trop Dis*. 2011; 5: e984. <https://doi.org/10.1371/journal.pntd.0000984> PMID: 21408126
 99. Schmieder R, Edwards R. Fast Identification and Removal of Sequence Contamination from Genomic and Metagenomic Datasets. Rodriguez-Valera F, editor. *PLoS One*. 2011; 6: e17288. <https://doi.org/10.1371/journal.pone.0017288> PMID: 21408061
 100. Wood DE, Salzberg SL. Kraken: ultrafast metagenomic sequence classification using exact alignments. *Genome Biol*. 2014; 15: R46. <https://doi.org/10.1186/gb-2014-15-3-r46> PMID: 24580807
 101. Mastretta-Yanes A, Arrigo N, Alvarez N, Jorgensen TH, Piñero D, Emerson BC. Restriction site-associated DNA sequencing, genotyping error estimation and de novo assembly optimization for population genetic inference. *Mol Ecol Resour*. 2015; 15: 28–41. <https://doi.org/10.1111/1755-0998.12291> PMID: 24916682
 102. Paris JR, Stevens JR, Catchen JM. Lost in parameter space: a road map for stacks. Johnston S, editor. *Methods Ecol Evol*. 2017; 8: 1360–1373. <https://doi.org/10.1111/2041-210X.12775>
 103. Catchen J, Hohenlohe PA, Bassham S, Amores A, Cresko WA. Stacks: an analysis tool set for population genomics. *Mol Ecol*. 2013; 22: 3124–40. <https://doi.org/10.1111/mec.12354> PMID: 23701397
 104. Danecek P, Auton A, Abecasis G, Albers CA, Banks E, DePristo MA, et al. The variant call format and VCFtools. *Bioinformatics*. 2011; 27: 2156–2158. <https://doi.org/10.1093/bioinformatics/btr330> PMID: 21653522
 105. Money D, Gardner K, Migicovsky Z, Schwaninger H, Zhong G-Y, Myles S. LinkImpute: Fast and Accurate Genotype Imputation for Nonmodel Organisms. G3 (Bethesda). 2015; 5: 2383–90. <https://doi.org/10.1534/g3.115.021667> PMID: 26377960
 106. Bradbury PJ, Zhang Z, Kroon DE, Casstevens TM, Ramdoss Y, Buckler ES. TASSEL: software for association mapping of complex traits in diverse samples. *Bioinformatics*. 2007; 23: 2633–2635. <https://doi.org/10.1093/bioinformatics/btm308> PMID: 17586829
 107. GOUDET J. hierfstat, a package for r to compute and test hierarchical F-statistics. *Mol Ecol Notes*. 2005; 5: 184–186. <https://doi.org/10.1111/j.1471-8286.2004.00828.x>
 108. Paradis E. pegas: an R package for population genetics with an integrated-modular approach. *Bioinformatics*. 2010; 26: 419–420. <https://doi.org/10.1093/bioinformatics/btp696> PMID: 20080509
 109. R Development Core Team. R: A language and environment for statistical computing. Vienna, Austria: R Foundation for Statistical Computing; 2016. Available: <http://www.r-project.org>
 110. Adamack AT, Gruber B. PopGenReport: Simplifying basic population genetic analyses in R. *Methods Ecol Evol*. 2014; 5: 384–387. <https://doi.org/10.1111/2041-210X.12158>
 111. Bilton TP, McEwan JC, Clarke SM, Brauning R, van Stijn TC, Rowe SJ, et al. Linkage disequilibrium estimation in low coverage high-throughput sequencing data. *Genetics*. 2018; 209: 389–400. <https://doi.org/10.1534/genetics.118.300831> PMID: 29588288

112. Saitou N, Nei M. The neighbor-joining method: a new method for reconstructing phylogenetic trees. *Mol Biol Evol.* 1987; 4: 406–425. <https://doi.org/10.1093/oxfordjournals.molbev.a040454> PMID: 3447015
113. Paradis E, Schliep K. ape 5.0: an environment for modern phylogenetics and evolutionary analyses in R. Schwartz R, editor. *Bioinformatics.* 2019; 35: 526–528. <https://doi.org/10.1093/bioinformatics/bty633> PMID: 30016406
114. Jombart T, Devillard S, Balloux F. Discriminant analysis of principal components: a new method for the analysis of genetically structured populations. *BMC Genet.* 2010; 11: 94. <https://doi.org/10.1186/1471-2156-11-94> PMID: 20950446
115. Jombart T. adegenet: a R package for the multivariate analysis of genetic markers. *Bioinformatics.* 2008; 24: 1403–5. <https://doi.org/10.1093/bioinformatics/btn129> PMID: 18397895
116. Nei M. Analysis of gene diversity in subdivided populations. *Proc Natl Acad Sci U S A.* 1973; 70. <https://doi.org/10.1073/pnas.70.12.3321> PMID: 4519626
117. Benjamini Y, Hochberg Y. Benjamini-1995.pdf. *Journal of the Royal Statistical Society B.* 1995. pp. 289–300. <https://doi.org/10.2307/2346101>
118. Briec MSO, Ono K, Drinan DP, Naish KA. Integration of Random Forest with population-based outlier analyses provides insight on the genomic basis and evolution of run timing in Chinook salmon (*Oncorhynchus tshawytscha*). *Mol Ecol.* 2015; 24: 2729–2746. <https://doi.org/10.1111/mec.13211> PMID: 25913096
119. Laporte M, Pavey SA, Rougeux C, Pierron F, Lauzent M, Budzinski H, et al. RAD sequencing reveals within-generation polygenic selection in response to anthropogenic organic and metal contamination in North Atlantic Eels. *Mol Ecol.* 2016; 25: 219–237. <https://doi.org/10.1111/mec.13466> PMID: 26562221
120. Briec MSO, Waters CD, Drinan DP, Naish KA. A practical introduction to Random Forest for genetic association studies in ecology and evolution. *Mol Ecol Resour.* 2018; 18: 755–766. <https://doi.org/10.1111/1755-0998.12773> PMID: 29504715
121. Forester BR, Lasky JR, Wagner HH, Urban DL. Comparing methods for detecting multilocus adaptation with multivariate genotype-environment associations. *Mol Ecol.* 2018; 27: 2215–2233. <https://doi.org/10.1111/mec.14584> PMID: 29633402
122. Whitlock MC, Lotterhos KE. Reliable detection of loci responsible for local adaptation: Inference of a null model through trimming the distribution of F_{ST} . *Am Nat.* 2015; 186: S24–S36. <https://doi.org/10.1086/682949> PMID: 26656214
123. Flanagan SP, Jones AG. Constraints on the F_{ST} –Heterozygosity Outlier Approach. *J Hered.* 2017; 108: 561–573. <https://doi.org/10.1093/jhered/esx048> PMID: 28486592
124. Breiman L. Random Forests. *Mach Learn.* 2001; 45: 5–32. <https://doi.org/10.1023/A:1010933404324>
125. Liaw A, Weiner M. Classification and Regression by randomForest. In: *R news* 2(3) [Internet]. 2002 pp. 18–22. Available: https://www.r-project.org/doc/Rnews/Rnews_2002-3.pdf
126. Holliday JA, Wang T, Aitken S. Predicting Adaptive Phenotypes From Multilocus Genotypes in Sitka Spruce (*Picea sitchensis*) Using Random Forest. 2012. <https://doi.org/10.1534/g3.112.002733> PMID: 22973546
127. Legendre P, Legendre L. Canonical analysis. *Developments in Environmental Modelling.* 2012. pp. 625–710. <https://doi.org/10.1016/B978-0-444-53868-0.50011-3>
128. Oksanen J. Multivariate Analysis of Ecological Communities in R: vegan tutorial. 2015. Available: <http://cc.oulu.fi/~jarioksa/opetus/metodi/vegantutor.pdf>
129. Oksanen J, Guillaume Blanchet F, Friendly M, Kindt R, Legendre P, McGlinn D, et al. vegan: Community Ecology Package. 2019. Available: <https://cran.r-project.org/package=vegan>
130. Forester BR, Jones MR, Joost S, Landguth EL, Lasky JR. Detecting spatial genetic signatures of local adaptation in heterogeneous landscapes. *Mol Ecol.* 2016; 25: 104–120. <https://doi.org/10.1111/mec.13476> PMID: 26576498
131. Capblancq T, Luu K, Blum MGB, Bazin E. Evaluation of redundancy analysis to identify signatures of local adaptation. *Mol Ecol Resour.* 2018; 18: 1223–1233. <https://doi.org/10.1111/1755-0998.12906> PMID: 29802785
132. Hijmans RJ, Van Etten J. raster: Geographic analysis and modeling with raster data. *Comprehensive R Archive Network (CRAN)*; 2012. Available: <https://cran.r-project.org/web/packages/raster/raster.pdf>
133. Mantel N. The Detection of Disease Clustering and a Generalized Regression Approach. *Cancer Res.* 1967; 27: 209–220. PMID: 6018555
134. Goslee SC, Urban DL. The ecodist Package for Dissimilarity-based Analysis of Ecological Data. *J Stat Softw.* 2007; 22: 1–19. <https://doi.org/10.18637/jss.v022.i07>

135. Clarke RT, Rothery P, Raybould AF. Confidence limits for regression relationships between distance matrices: Estimating gene flow with distance. *J Agric Biol Environ Stat.* 2002; 7: 361–372. <https://doi.org/10.1198/108571102320>
136. Alexander DH, Novembre J, Lange K. Fast model-based estimation of ancestry in unrelated individuals. *Genome Res.* 2009; 19: 1655–1664. <https://doi.org/10.1101/gr.094052.109> PMID: 19648217
137. Meirmans PG, Hedrick PW. Assessing population structure: FST and related measures. *Mol Ecol Resour.* 2011; 11: 5–18. <https://doi.org/10.1111/j.1755-0998.2010.02927.x> PMID: 21429096
138. Meirmans PG, Van Tienderen PH. genotype and genodive: two programs for the analysis of genetic diversity of asexual organisms. *Mol Ecol Notes.* 2004; 4: 792–794. <https://doi.org/10.1111/j.1471-8286.2004.00770.x>
139. Cohen J. A power primer. *Psychol Bull.* 1992; 112: 155–159. <https://doi.org/10.1037//0033-2909.112.1.155> PMID: 19565683
140. Scrucca L. GA: A package for genetic algorithms in R. *J Stat Softw.* 2013; 53: 1–37. <https://doi.org/10.18637/jss.v053.i04>
141. Fouss F, Pirotte A, Renders JM, Saerens M. Random-walk computation of similarities between nodes of a graph with application to collaborative recommendation. *IEEE Trans Knowl Data Eng.* 2007; 19: 355–369. <https://doi.org/10.1109/TKDE.2007.46>
142. Shah VB, Mcrae B. Circuitscape: A Tool for Landscape Ecology. In: Varoquaux G, Vaught T, Millman J, editors. *Proceedings of the 7th Python in Science Conference (SciPy 2008)*. 2008. pp. 62–66. Available: https://circuitscape.org/pubs/Shah_McRae_Circuitscape_Python_Scipy08.pdf